WEATHERSAFE

SAFETY ENHANCEMENT UNDER ADVERSE WEATHER CONDITIONS THROUGH IMPROVED ADAS/AD ROBUSTNESS

Deliverable 3.0

Assessment of ADAS/AD performances under Adverse Weather Conditions

Project Name	WeatherSafe	
Dissemination level	Public/ Consortium	
Author	Lucas Dulewicz	VUFO
Co-Author	Theresa Weber	VUFO
Issue date		
Reviewer	Thomas Unger	
Keywords	Simulation, Accident, Weather, Adverse	
Version	1.2	

EXECUTIVE SUMMARY

The "WeatherSafe" project aims to analyse the impact of adverse weather conditions (AWC) on traffic accidents in Germany and Europe, focusing on the effectiveness of Advanced Driver Assistance Systems (ADAS). Therefor a selection of the top 5 accident scenarios is conducted. Based on these scenarios the effectiveness of different ADAS configurations in AWC is determined by re-simulation of the accidents. For this re-simulation influences from AWC on the ranges of different sensors are quantified in order to parameterize the models for the re-simulation of the accident scenarios. The results of the different ADAS configurations are used to quantify the influence of friction detection and sensor perception on the ADAS performance in AWC.

REVISION HISTORY

Revision	Date	Description, updates and changes	Status
1.1	06.08.2025	Collision speeds added in 2.4 TTC grouped by collision occurrence added in 3.2.2 Minor changes in text/wording	Draft
1.2	22.05.2026	Addition of KSI evaluation after exclusion of loss of control accident scenarios within chapter 2.3.	Approved

ABBREVIATIONS

ADAS	Advanced Driver Assistance System
AW	Adverse Weather
AWC	Adverse Weather Conditions
ESC	Electronic Stability Control
GIDAS	German In-Depth Accident Study
LOC	Loss of control
PCM	Pre-Crash-Matrix
RSSI	Received Signal Strength Indicator
V2V	Vehicle to vehicle communication
WP	Work Package

TABLE OF CONTENTS

EXECUTIVE SUMMARY 2
REVISION HISTORY 3
ABBREVIATIONS 4
TABLE OF CONTENTS 5
1. INTRODUCTION 6
1.1 MAIN GOALS AND METHODOLOGY OF WP3 6
1.2 RELATION TO THE OTHER WORK PACKAGES 6
2. DEFINITION OF AWC ANALYSIS SCOPE AND PARAMETERS 7
2.1 ANALYSIS SCOPE: CURRENT STATE OF THE SCENARIO ANALYSIS 7
2.2 FURTHER ANALYSIS OF THE ACCIDENT DATA 9
2.3 FINAL TEST SCENARIO SELECTION 14
2.4 GIDAS PRE-CRASH-MATRIX 17
3. RE-SIMULATION OF SELECTED AW SCENARIOS 22
3.1 RE-SIMULATION METHODOLOGY 22
3.1.1 Modelling of Sensors 22
3.1.2 Influence of AWC on Sensors 23
3.1.3 Configurations of ADAS 25
3.1.4 V2V modelling 26
3.2 RESULTS OF RE-SIMULATION 29
3.2.1 Exemplary single case results 29
3.2.2 Overall result of ADAS configurations 30
3.2.3 Isolated effect of friction detection 35
3.2.4 Isolated effect of perception 36
3.2.5 Effect of V2V 37
4. SUMMARY AND OUTLOOK 38
5. LIST OF ILLUSTRATIONS 40
6. LIST OF TABLES 41
7. REFERENCES 42

1. Introduction

Weather conditions play a crucial role in shaping a driver's visibility and overall driving experience. Factors such as precipitation, sun glare or wet and icy roads can significantly impact driving safety. Modern vehicles are equipped with various assistance systems designed to assess and respond to different traffic situations. However, it is important to consider whether these sensors and their integrated systems are also influenced by weather conditions. If they are, how do these changes affect their performance, and what potential consequences might arise? Ensuring safe driving in all weather conditions is a complex challenge that raises many unanswered questions, which this project aims to explore. This study focuses on analysing weather conditions at the time of traffic accidents across Europe and examining the impact of adverse weather (AW) on road safety.

1.1 Main goals and methodology of WP3

This work package (WP3) focuses on analysing the safety benefits of ADAS in mitigating the effects of adverse weather conditions (AWC) on driving. By integrating the findings from previous work packages (WP1 and WP2), this study aims to define critical scenarios and key variables necessary for assessing safety improvements. A virtual testing approach will be employed to simulate these scenarios, enabling a comprehensive evaluation of potential risk reductions. The analysis will be conducted in two phases: first, by defining the scope and parameters of safety benefits analysis, and second, by re-simulating selected scenarios to assess improvements in safety performance. The final deliverable will compile the methodology, findings, and potential safety gains, providing insights into the most relevant cases for further study. This work will contribute to refining and enhancing ADAS capabilities for safer driving in challenging weather conditions.

1.2 Relation to the other work packages

WP3 builds directly on the outcomes of WP1 and WP2, and in turn informs WP4. In WP1 (“Accident Data Study”), the project team identified which accident scenarios are most relevant under AWC and pinpoints the variables that define those scenarios. In WP2 (“Phenomenon Characterization”), meteorological phenomena and their key parameters were specified, providing a detailed picture of the weather factors contributing to critical situations.

Using these inputs, WP3 (“Safety Benefits Analysis”) evaluates how ADAS can mitigate the risks highlighted by WP1 and WP2. WP3’s virtual testing approach relies on both the accident data (WP1) and the weather characterizations (WP2) to simulate realistic driving scenarios under challenging conditions. This two-phase analysis—defining the scope and parameters of safety benefits, then re-simulating selected scenarios—quantifies potential improvements in road safety when ADAS is deployed.

Finally, WP4 (“Reproducibility Study”) takes WP3’s findings and assesses how well they can be reproduced through physical or simulated tests. By reviewing existing testing infrastructures and tools, WP4 determines whether these systems can replicate the weather and accident scenarios defined in WP1, WP2, and WP3, or whether new approaches are needed. Through this workflow, WP3 serves as the critical link between identifying real-world accident/weather factors (WP1 and WP2) and confirming how to replicate and validate ADAS performance in test settings (WP4).

WP5 (“Test and Assessment Procedures”) is dedicated to establishing assessment guidelines for the use cases identified in earlier work packages. It involves defining test scenarios, protocols, and evaluation methods to reliably assess system performance, ultimately delivering a comprehensive report on testing and assessment methodologies. Thus, WP3 not only provides the analytical foundation for understanding the safety impacts of ADAS under AW but also directly informs WP5’s efforts to create standardized testing and assessment procedures.

2. Definition of AWC analysis scope and parameters

Chapter 2, "Definition of AWC analysis scope and parameters," establishes the analytical framework for assessing AWC in traffic accident scenarios. This chapter is divided into two main sections. Subchapter 2.1, "Analysis Scope: Current state of the scenario analysis," reviews the existing body of work, presenting a detailed flowchart that maps out the methodologies and key findings from the investigation of accident databases and AW associations. This section provides a clear depiction of how accident data has been classified and interpreted, laying the groundwork for further analysis. Subchapter 2.2, "Further analysis of the accident data," then builds on these initial insights by outlining additional criteria and variables for refining the selection of critical scenarios. Together, these sections define the scope and parameters essential for a comprehensive evaluation of AWC impacts on road safety. That information is gathered in subchapter 2.3 and conclude to a final top five scenario selection, which can be used for the following re-simulation.

2.1 Analysis scope: Current state of the scenario analysis

The flowchart in Figure 1 provides an overview of the scenario analysis conducted in the project, focusing on the role of AW in traffic accidents. It demonstrates how statistical accident data has been examined, particularly using the German In-depth Accident Study (abbr.: GIDAS) database, to assess the relevance of weather conditions in accident scenarios.

The analysis starts with an evaluation of multiple statistical accident data, noting that most datasets record weather as a circumstance, while DESTATIS recognizes weather as a causative factor. Summarizing, the statistical data shows the higher relevance of rainy weather as a circumstance and an accident causation. The highest relevance belongs to dry or sunny weather which can contribute to AW as well, due to sun glare.
A thorough analysis of the GIDAS database is performed, reviewing 45,434 fully documented accidents, of which 32,441 involve at least one passenger vehicle. Out of these, 9,902 accidents (21.8 %) are associated with AWC. These incidents are classified into three groups: 0.5 % (53 cases) are directly caused by AW, primarily due to snowy/icy roads (45 %), sun glare (30 %), or wet roads (15 %); 16.4 % (1,619 cases) had AW as a contributing factor, with wet roads (36 %), snowy/icy conditions (31 %), and sun glare (22%) being the most common; and 83.1 % (8,230 accidents) featured weather as a circumstantial condition, mostly occurring in dry conditions (86.3 %), followed by rain (11.8 %) and snow (1.3%). The analysis culminated in the identification of the top five accident scenarios critically influenced by AWC.

These results provide a comprehensive foundation for subsequent work on advanced driver assistance systems and the development of testing protocols. This work represents a significant step in WP1 and WP2, defining accident scenarios and characterizing meteorological conditions. The findings serve as the basis for WP3, where ADAS performance will be analysed in these conditions. The results will also inform WP4 and WP5 by defining relevant test scenarios and evaluation procedures.

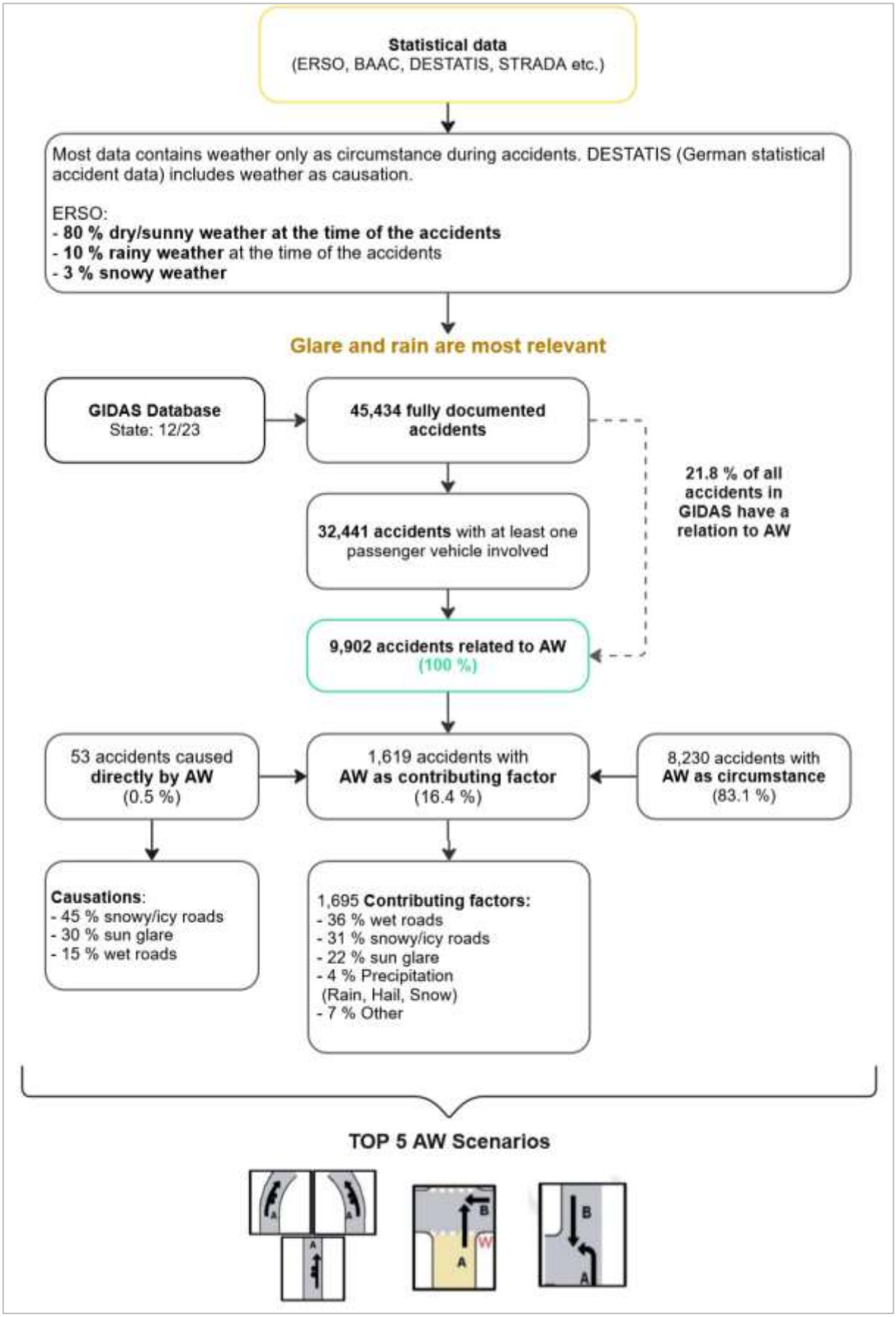

Figure 1 - Analysis of weather parameters and results of WP1 [1]

2.2 FURTHER ANALYSIS OF THE ACCIDENT DATA

The following chapter includes further accident analysis steps which are part of the WP3. These are part of the discussion of the project partners und should clarify conclusions. All these analyses are done within the GIDAS database which defines the scenario selection and includes AW accident cases, which are already defined in WP1.

Variable name:	SCHLEU
Start of documentation in GIDAS:	1999
Description:	Indicates if the participant had a problem with skidding during the accident, defining if it is over- or understeering.
Evaluation level:	Participant level

The variable described above includes the information about the presence of skidding and what kind of skidding is happening at the time of the loss of control (abbr.: LOC) accident.
This flowchart presents an analysis of the 1,853 LOC accident scenarios, categorizing them by the presence of skidding, the type of skidding, and the involvement of Electronic Stability Control (abbr.: ESC) in each case.

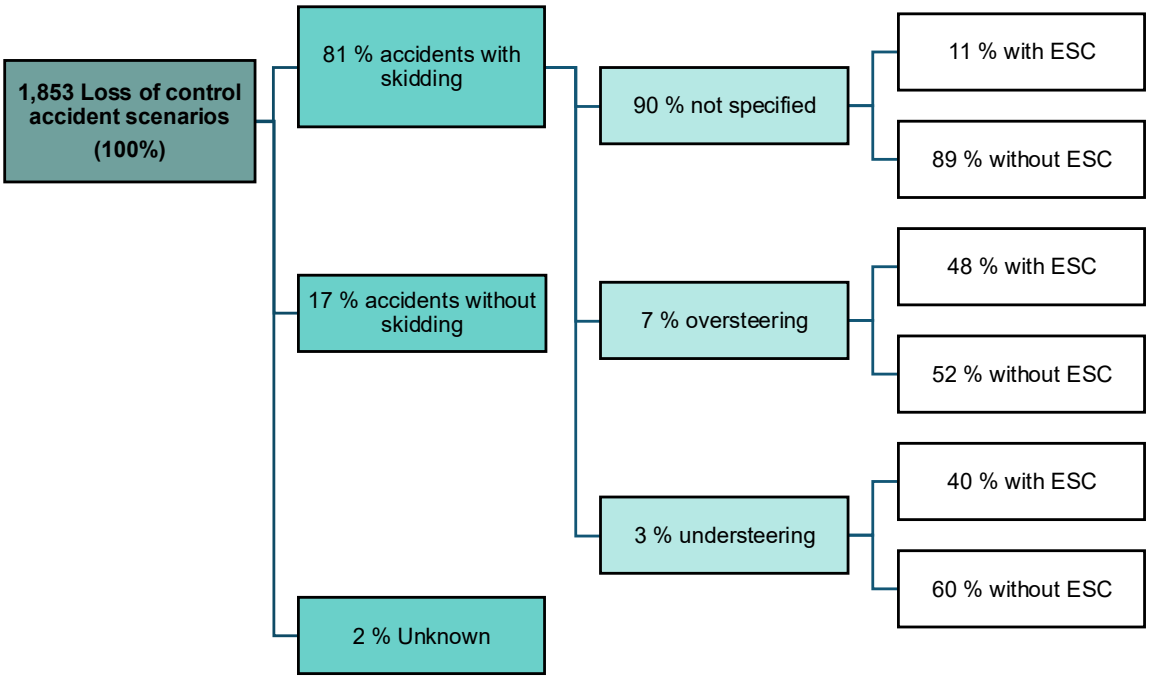

Figure 2 - LOC accidents and their presence of skidding

First, the accidents are divided into three main categories: 81 % of the accidents involve skidding, while the remaining 17 % do not involve skidding and 2 % are unknown.
Among the 81 % of accidents that involve skidding, the majority, 90 %, do not specify the type of skidding (either oversteering or understeering). Within this unspecified group, 11 % of the accidents occur with ESC, and 89 % occur without ESC. Additionally, 7 % of the skidding accidents are due to oversteering, with 48 % occurring with ESC and 52 % without ESC. Another 3 % of the skidding accidents are due to understeering, where 40 % occur with ESC and 60 % occurred without ESC.
Finally, for the 18.8 % of accidents that do not involve skidding, there are no further breakdowns provided in the flowchart.
This chart highlights that most LOC accidents are skidding-related and those occurred without ESC, especially in cases where the type of skidding is unspecified. It underscores the potential importance of ESC in preventing LOC accidents. This topic underlines that it is not as relevant to include LOC accidents in the scenario selection, due to a high prevention possibility through ESC in the future.

This flowchart examines 1,503 LOC accident scenarios involving skidding, breaking them down by different road surface conditions and the presence or absence of precipitation.

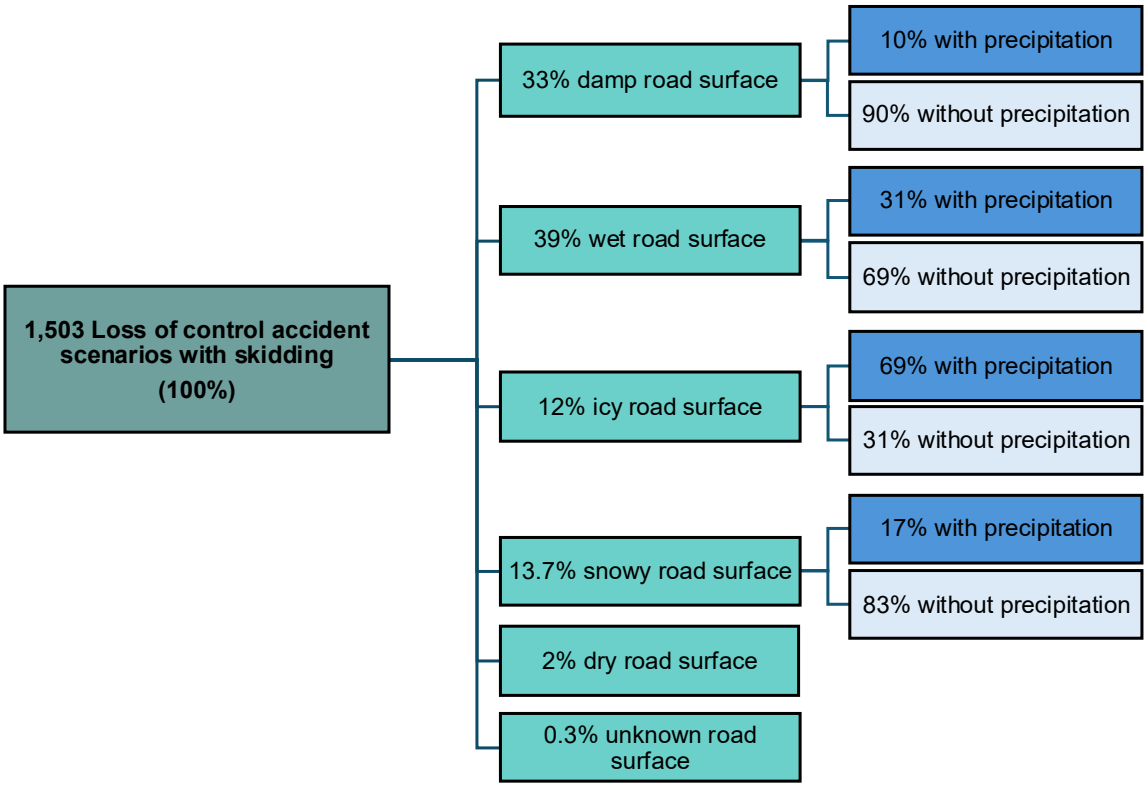

Figure 3 - Distribution of road surface conditions and precipitation in LOC accidents

A significant portion of the accidents, 33 %, took place on damp road surfaces. Of these, 10 % occurred during precipitation, while the remaining 90% happened without any precipitation. Similarly, 39 % of the accidents occurred on wet road surfaces, with 31 % of them taking place during precipitation and 69 % without precipitation.
For accidents on icy road surfaces, which accounted for 12 % of the total, 69 % of the incidents occurred during precipitation, while 31 % happened without it. On snowy road surfaces, which made up 13.7 % of the accidents, 17 % occurred during precipitation and 83 % without precipitation.
There are also 2 % of the accidents on dry road surfaces, but this category did not provide further breakdowns based on precipitation. Additionally, 0.3 % of the accidents occurred on unknown road surfaces.
The flowchart highlights that while skidding accidents are most common on wet and damp roads, most of these accidents occurred without active precipitation at the time of the accident.

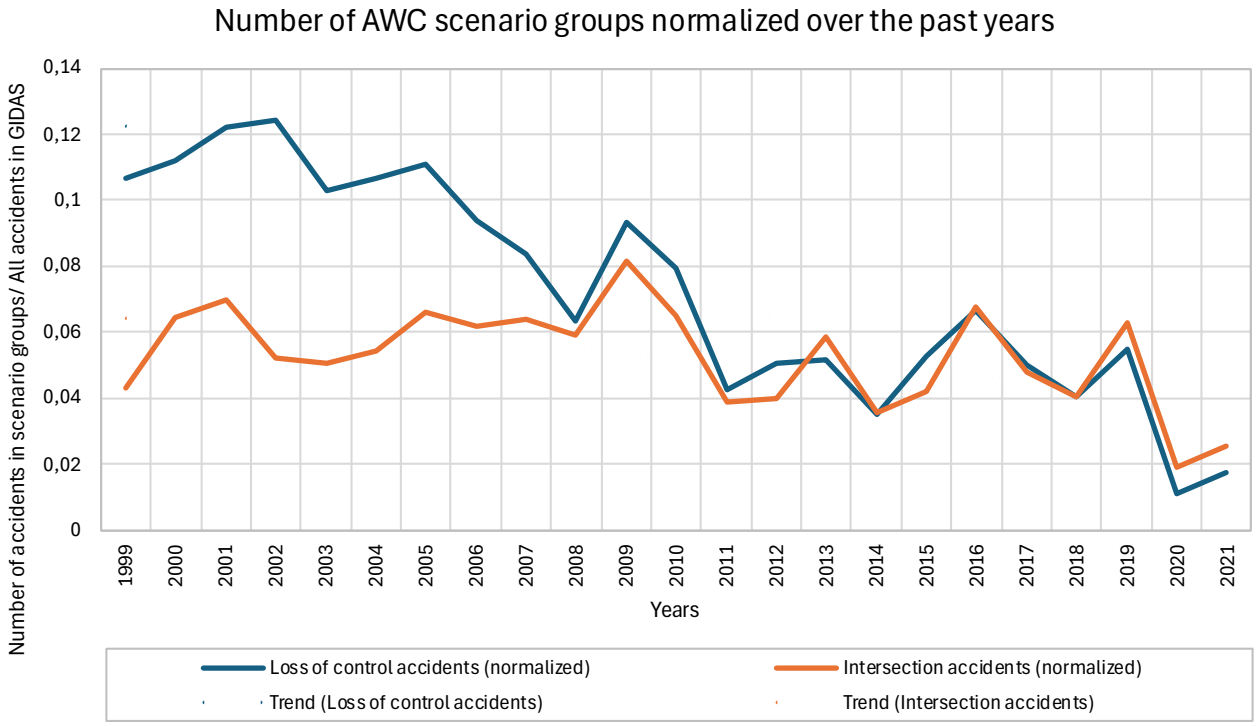

Figure 4 - Number of LOC accidents under AWC over the past years

The chart illustrates the temporal development of the two most common accident scenario groups under AWC - LOC and Intersection Accidents - based on normalized data from GIDAS. The data spans from 1999 to 2021 and presents the share of these scenario groups in relation to all accidents recorded in GIDAS for each year.
The blue line represents LOC accidents, while the orange line corresponds to intersection accidents. Both are normalized to allow comparison across years. Over the analysed period, a significant downward trend can be observed for both accident types, as indicated by their respective dotted trendlines. However, the decline in LOC accidents is more pronounced, showing a sharper decrease in frequency compared to intersection accidents.
In the early 2000s, LOC accidents comprised up to approximately 12 to 13 % of all recorded accidents in GIDAS, while intersection accidents accounted for around 6 to 7 %. From 2009 onwards, the proportion of LOC accidents began to fluctuate more dramatically but continued to decline overall, reaching below 2 % in 2021. Intersection accidents, on the other hand, exhibited a steadier decline and less pronounced variation, remaining between 4 to 6% in most years.
These findings suggest that while both scenario types have become less prevalent over the past two decades - likely due to advancements in vehicle safety systems and infrastructure - the reduction in LOC accidents under AWC is particularly substantial. This may reflect the growing effectiveness of stability and driver-assist systems in mitigating scenarios involving vehicle control loss on slippery or hazardous road surfaces.

Overall, the chart reveals a strong downward trend in the number of LOC accidents in comparison to the intersection accidents under AWC, especially in the later years. This analysis underlines as well to exclude the LOC accident type since the final scenario selection, because the general relevancy seems to decrease over the years and intersection scenarios are more relevant.

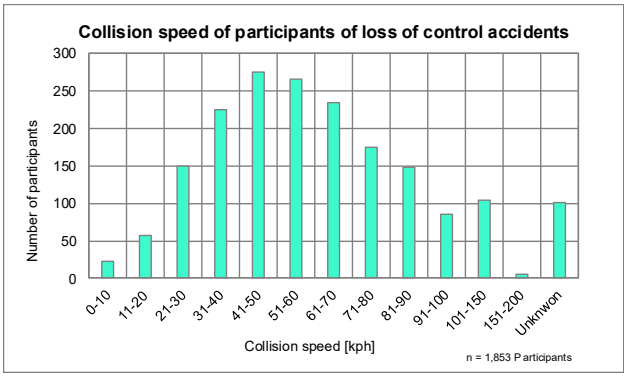

Figure 5 - Collision speed of participants of loss of control accidents

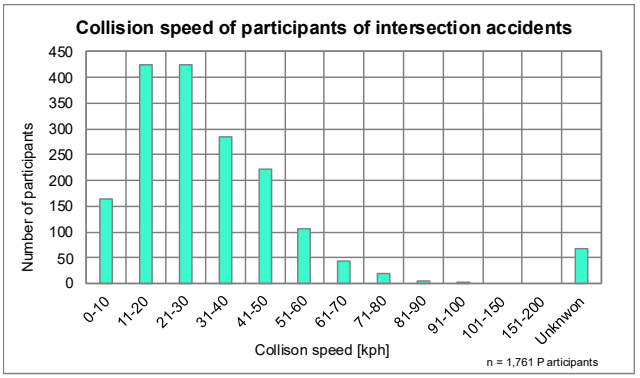

Figure 6 - Collision speed of participants of intersection accidents

Another point which underlines the tendency to not include LOC accidents, is the accident causation "speeding". The following two charts show the collision speeds of loss of control accidents and in contrast the collision speed of intersection accidents. Those speeds are extracted to analyse the general velocity of the accident participants. The analysis shows that LOC accidents have quite higher collision speed than intersection accidents.

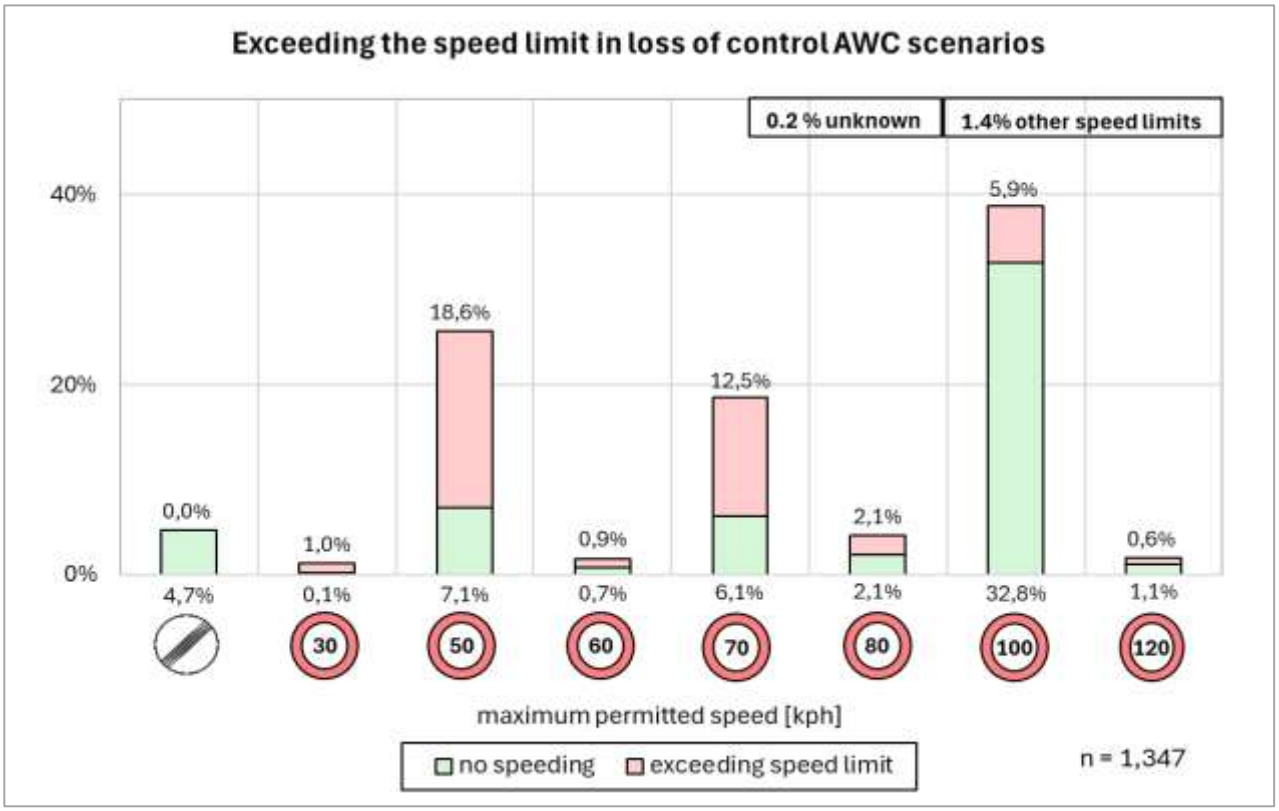

Figure 7 - Distribution of accidents which are caused by the participant exceeding the speed limit

The chart illustrates the distribution of speed compliance in LOC accident scenarios under AWC, focusing on the extent to which exceeding the speed limit contributed to such events. For the analysis the initial speeds from the reconstruction were used. These speeds represent the most probable speeds but are subject to inaccuracies. Based on the analysis of 1,347 LOC-AWC cases, the data is segmented by various maximum permitted speed limits (in km/h), ranging from 30 km/h to 120 km/h.

A key observation is that speeding is a significant contributing factor in LOC accidents, particularly in zones with speed limits of 50 km/h and 70 km/h. For 50 km/h zones, 18.6 % of LOC accidents occurred, with a substantial portion (approximately two-thirds) involving speeding. Similarly, in 70 km/h zones, 12.5 % of all LOC cases are recorded, and a notable share also involved excessive speed.

By contrast, in low-speed zones such as 30 km/h and 60 km/h, both the overall accident shares and the speeding-related portions are minimal, indicating that excessive speed is less of a factor in these areas. The highest proportion of LOC-AWC accidents occurred in 100 km/h zones (32.8 %), but interestingly, most of these incidents involved no speeding, suggesting other contributing factors such as road conditions or driver error at high speeds.

Additional data reveals that a small share of accidents occurred under unknown or other speed limits (1.6 % combined), and 4.7 % occurred in environments without an applicable speed limit (e.g., off-road or private areas).

In summary, while speeding is not the sole cause of LOC accidents, the data clearly shows that it plays a critical role, particularly in urban to semi-urban areas with speed limits between 50 and 70 km/h. These findings highlight the importance of speed management strategies and vehicle stability systems, especially under AWC, to mitigate LOC scenarios.

2.3 FINAL TEST SCENARIO SELECTION

The analysis in the subchapter 2.2 underline the declining relevancy of the analysis of LOC scenarios under AWC. The number of LOC accidents tend to decrease a lot more than the intersection accident scenarios (Figure 4). The goal of this project is to examine relevant AW scenarios and to give recommendations for possible test scenarios in the future. The guidelines for LOC scenarios are limited as they don't include a direct opponent and within this problematic the testing of ADAS could be more difficult. The reference for Automatic Emergency Braking or Adaptive Cruise Control testing systems would be missing. Therefor the decision within the consortium is made, to exclude LOC out of the top five AWC scenarios.

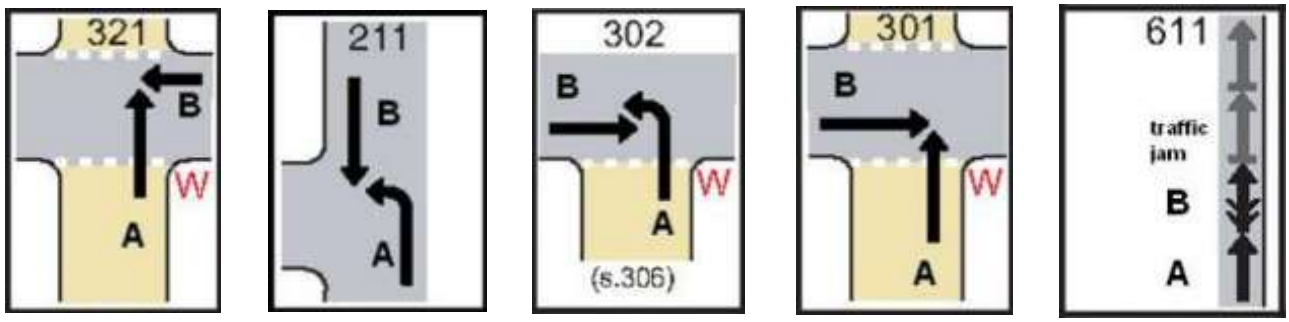

N = 580
Participant A wants to cross a priority road and has a conflict with participant B which comes from the right side.

N = 557
Participant A wants to cross a priority road and has a conflict with participant B which comes from the right side.

N = 475
Participant A wants to turn left onto a priority road has a conflict with participant B which comes from the left side.

N = 362
Participant A wants to cross a priority road and has a conflict with participant B which comes from the left side.

N = 343
This scenario includes a traffic jam. Participant B is braking. Participant A has a conflict with B from behind.

Figure 8 - Top five accident scenarios for re-simulation

These scenarios, illustrated in the figure, represent the most critical and recurrent accident configurations influenced by AW, excluding loss-of-control accidents. The selection process prioritized scenarios where AWC significantly affects driver behaviour, visibility, or vehicle interactions rather than those dominated by skidding or traction loss. These refined cases will serve as the foundation for the next phase of the study: the re-simulation.
The following chapter focuses on the re-simulation process, where these accident scenarios will be reconstructed in a virtual environment. By leveraging advanced simulation techniques, this analysis aims to assess the potential safety benefits of ADAS in mitigating risks under AWC. The findings will contribute to a deeper understanding of ADAS effectiveness and provide insights into refining future vehicle safety strategies.

The following Table 1 summarizes the detailed weather conditions during the top five AWC accident scenarios without LOC accidents. Road surface and the combination of precipitation and road surface still seem to have a quite similar and high share in all scenarios, although LOC accidents were excluded. Sun glare and sun glare in combination with road surface becomes a higher relevance with the exclusion of LOC accidents. This topic seems to be more important during intersection accident types, like the ones displayed below.

Table 1 - Detailed weather conditions during the top five AWC scenarios without LOC

Top 5 AWC-Scenarios	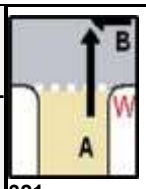 **321**	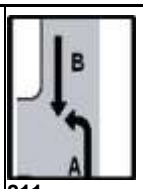 **211**	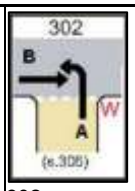 **302**	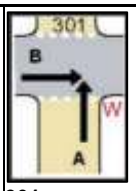 **301**	 **611**
Number of scenarios	N = 580	N = 557	N = 475	N = 362	N = 343
Road surface	46.2 %	37.9 %	46.9 %	41.4 %	42.6 %
Road surface + Precipitation	37.1 %	40.2 %	39.6 %	47.5 %	41.7 %
Sun Glare	14.0 %	20.5 %	11.8 %	9.4 %	13.4 %
Sun Glare + Road Surface	1.7 %	0.5 %	1.5 %	0.8 %	1.2 %
Precipitation	0.9%	0.4 %	0.2 %	0.3 %	0.3 %
Road Surface + Fog	0.0 %	0.5 %	0.0 %	0.6 %	0.0 %
Precipitation + Sun Glare + Road surface	0.2 %	0.0 %	0.0 %	0.0 %	0.3 %
Precipitation + Road Surface + Fog	0.0 %	0.0 %	0.0 %	0.0 %	0.3 %

Evaluation of top five KSI scenarios without LOC scenarios:

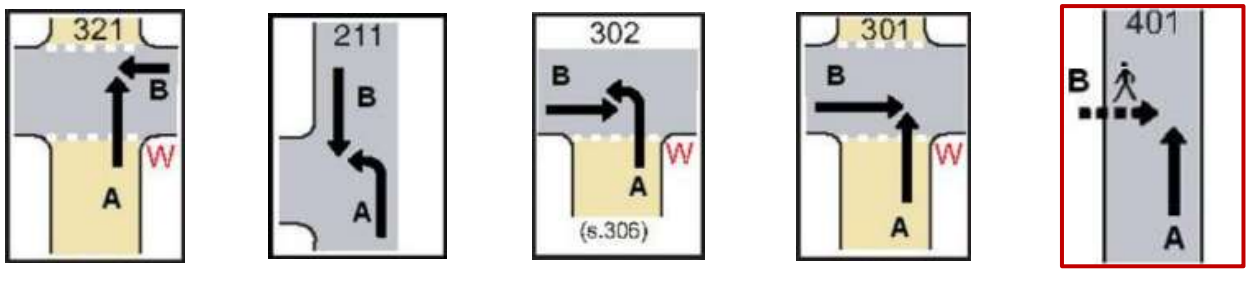

N = 147 Participant A wants to cross a priority road and has a conflict with participant B which comes from the right side.	**N = 135** Participant A wants to cross a priority road and has a conflict with participant B which comes from the right side.	**N = 117** Participant A wants to turn left onto a priority road has a conflict with participant B which comes from the left side.	**N = 92** Participant A wants to cross a priority road and has a conflict with participant B which comes from the left side.	**N = 63** This scenario includes a crossing pedestrian as participant B. Participant A has a conflict with B from the front.

Figure 9 - Top five AW KSI accident scenarios

If the focus is on the same scenarios but with accidents with at least one killed or severely injured persons involved in the accidents, the distribution changes a little. The accident type “611”, which was on the fifth place in the ranking in Figure 8, is replaced by **the accident type “401”.**
Accident scenarios involving a pedestrian become more relevant for AWC, when looked at more severe accidents.

Table 2 - Detailed weather conditions during the top five KSI scenarios without LOC

Top 5 AWC-Scenarios	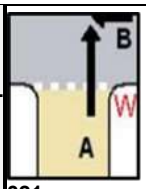 321	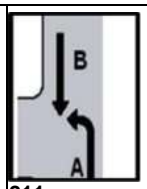 211	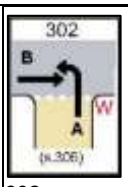 302	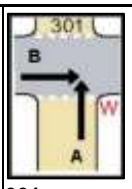 301	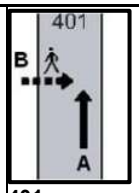 401
Number of scenarios	N = 147	N = 135	N = 117	N = 92	N = 63
Road surface	46.2 %	37.3 %	46.9 %	41.2 %	38.8 %
Road surface + Precipitation	37.1 %	40.2 %	39.6 %	47.5 %	56.3 %
Sun Glare	14.0 %	20.5 %	11.8 %	9.4 %	4.9 %
Sun Glare + Road Surface	1.7 %	0.5 %	1.5 %	0.8 %	0.0 %
Road Surface + Fog	0.0 %	1.1 %	0.0 %	0.8 %	0.0 %
Precipitation	0.9 %	0.4 %	0.2 %	0.3 %	0.0 %
Precipitation + Sun Glare + Road Surface	0.2 %	0.0 %	0.0 %	0.0 %	0.0 %

Table 2 summarizes the detailed weather conditions during the top five KSI accident scenarios. Road surface and the combination of precipitation and road surface still seem to have a quite similar and high share in all scenarios, as well as the higher proportion of sun glare as in Table 1.

2.4 GIDAS PRE-CRASH-MATRIX

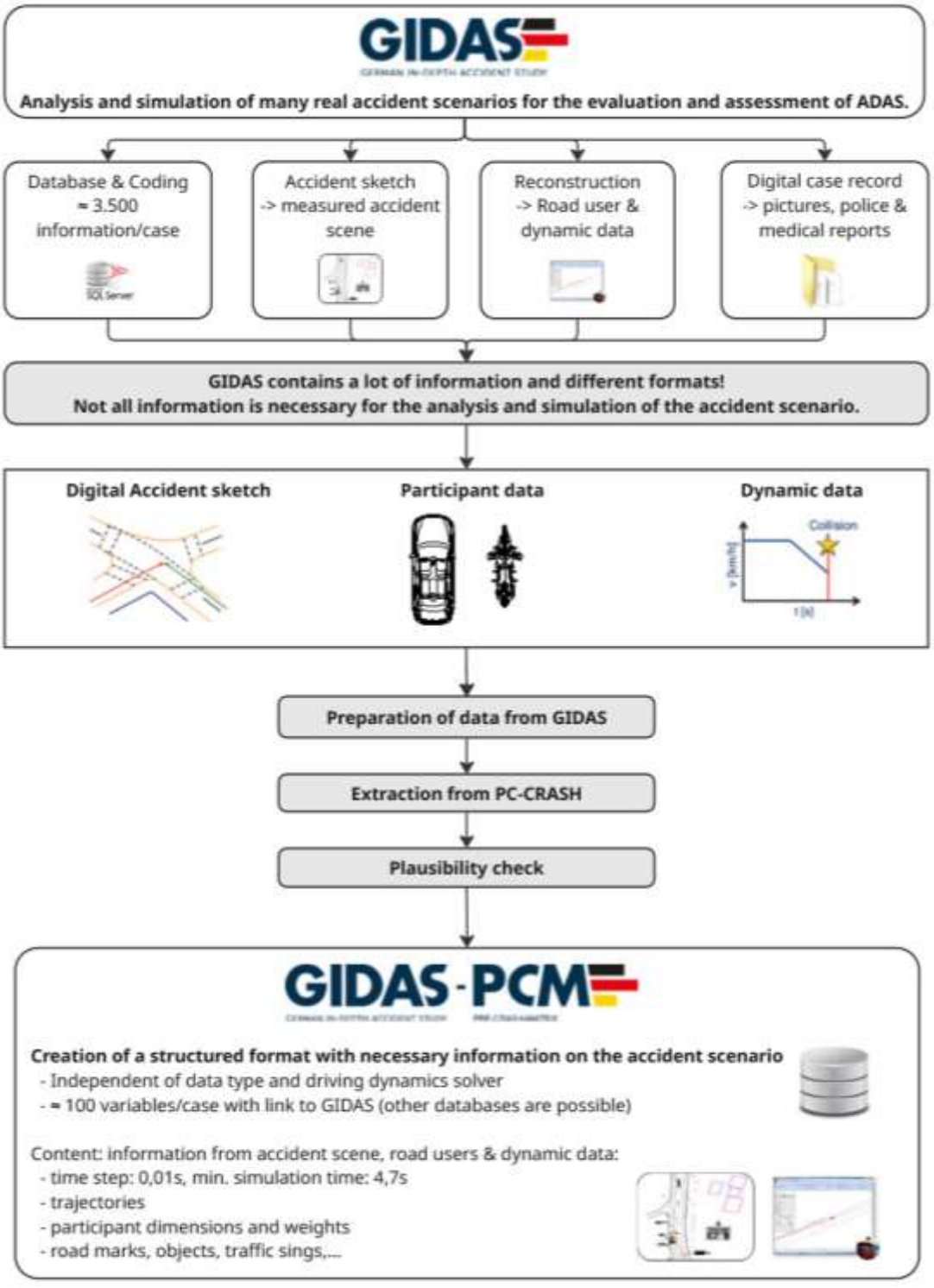

Figure - Creation process of the GIDAS-PCM

The GIDAS-PCM (abbr.: Pre-Crash Matrix) is a structured data format designed to provide essential information for accident scenario analysis and simulation, particularly for the assessment of ADAS. It integrates various data sources from GIDAS, including accident sketches, participant data, and dynamic parameters, to enable accurate reconstructions of real-world accidents.

The creation process begins with the collection of accident data, which includes digital accident sketches, participant information and dynamic data. These data are extracted from the GIDAS database and further processed through PC-Crash, a reconstruction software. A plausibility check ensures the accuracy of the extracted information before the data is formatted into GIDAS-PCM, making it compatible with driving simulation tools like IPG CarMaker.
The GIDAS-PCM contains approximately 100 variables per case, linking back to the GIDAS database. The dataset includes key accident scene elements such as trajectories, participant dimensions and weights, road markings, objects, and traffic signs. It operates with a 0.01-second time step and a minimum simulation time of 4.7 seconds, ensuring a detailed representation of the accident sequence.

However, the GIDAS-PCM has specific restrictions:

- It only includes accidents with case status = 4 (verified coding and reconstruction).
- Only the first collision of an accident is considered.
- Only participants with a stable driving condition are included.
- It accounts for specific road users, including passenger cars, trucks, pedestrians, bicycles, motorcycles, and objects.
- It does not include traffic or environmental influences, limiting its ability to model complex multi-vehicle interactions or AWC.

Despite these restrictions, the GIDAS-PCM serves as a valuable tool for analysing pre-crash scenarios, supporting the development and validation of ADAS technologies, and enhancing traffic safety research.

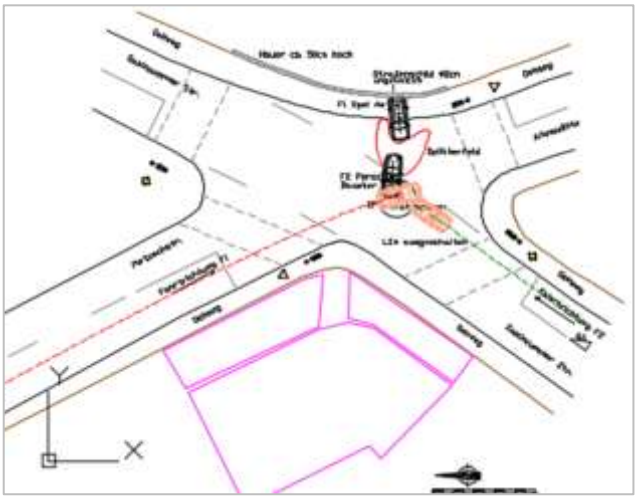

Figure 10 - Traffic accident scenario as first sketch



Figure 11 - Simulated accident scenario as trajectory in the PCM

Figure 10 illustrates a typical accident scene sketch from the GIDAS database, depicting the exact positioning of vehicles, road layout, and relevant environmental markings. Such sketches are crucial for understanding the initial conditions and context of each accident scenario. From this raw accident data, the scene is then digitized and converted into a trajectory-based representation within the PCM framework, as demonstrated in Figure 11. Here, the paths of the involved vehicles are translated into coordinate data points, creating an abstract and standardized depiction of the scenario. This allows for simulations and analyses that are independent of specific data formats and vehicle dynamics solvers.

The updated accident scenario data from the GIDAS-PCM refines the selection of the top five accident configurations influenced by AWC. The revised numbers indicate the specific occurrence frequency of each scenario within the dataset, with scenario 321 being the most frequent (n = 299) and scenario 611 the least frequent (n = 152). This dataset provides a more precise basis for subsequent re-simulation efforts, ensuring that the most representative and safety-relevant cases are analysed in detail.

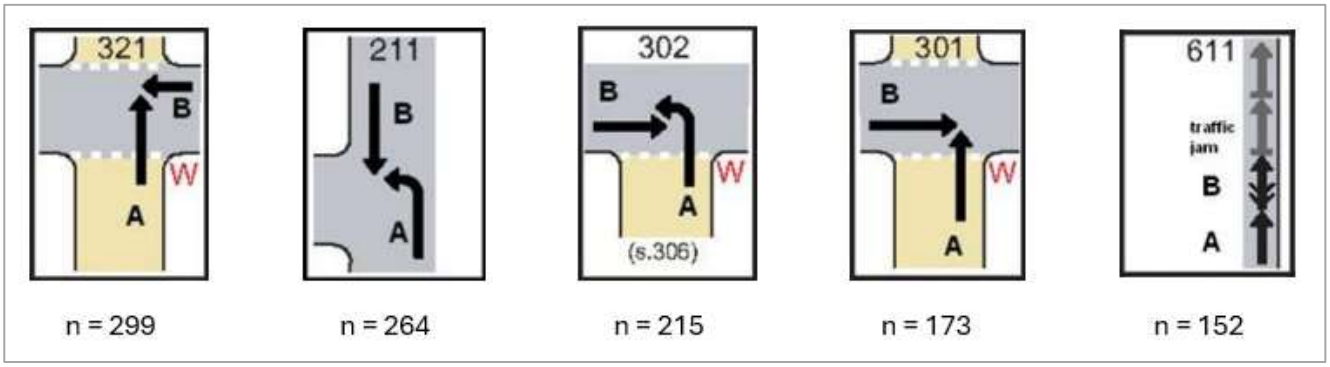

Figure 12 - Top five AWC scenarios and their number of cases in the GIDAS-PCM

The next three charts examine the distribution of AW in the PCM-AW-scenarios. The displayed weather conditions are not included in the PCM but are extracted from GIDAS directly.

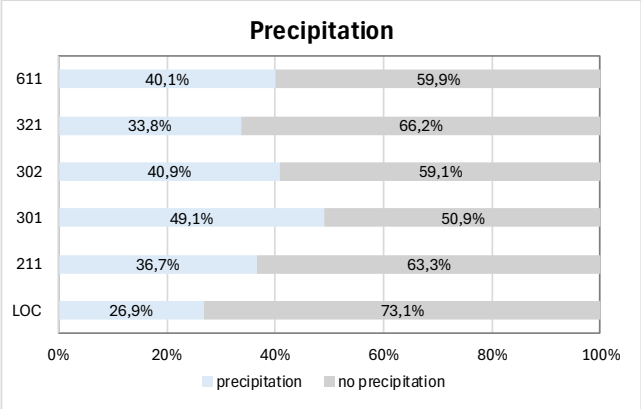

Figure 13 - Distribution of precipitation in the top five PCM scenarios

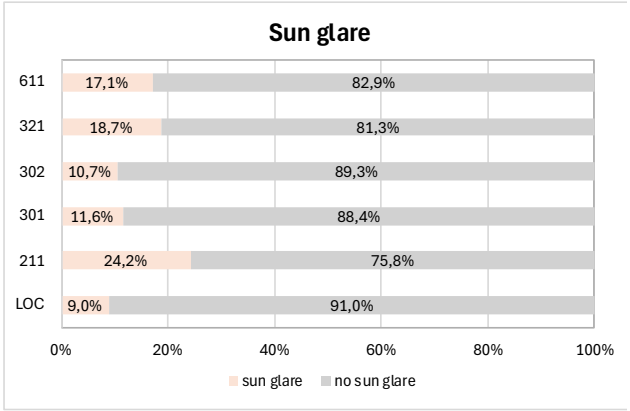

Figure 14 - Distribution of sun glare in the top five PCM scenarios

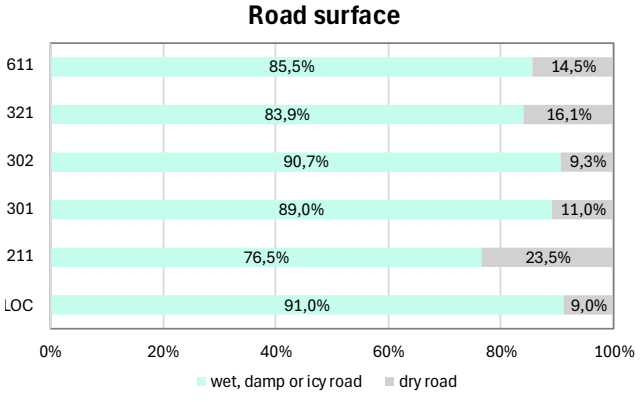

Figure 15 - Distribution of road surface conditions in the top five PCM scenarios

The three charts provide an overview of the environmental conditions affecting the top five PCM accident scenarios, specifically focusing on road surface conditions, precipitation, and sun glare. Figure 15 illustrates the distribution of road surface conditions, distinguishing between wet, damp, or icy roads and dry roads. Most scenarios involve non-dry road conditions, indicating the significant influence of AW on accident occurrence.

Figure 13 highlights the presence of precipitation in these scenarios, with a substantial portion of accidents occurring under rainy or snowy conditions, further reinforcing the role of AW factors. Figure 14 examines the effect of sun glare, showing that certain scenarios are notably affected by this factor, emphasizing its contribution to reduced visibility and accident risk. Collectively, these figures underscore the relevance of weather-related parameters in accident scenarios and provide essential insights for further analysis and countermeasure development.

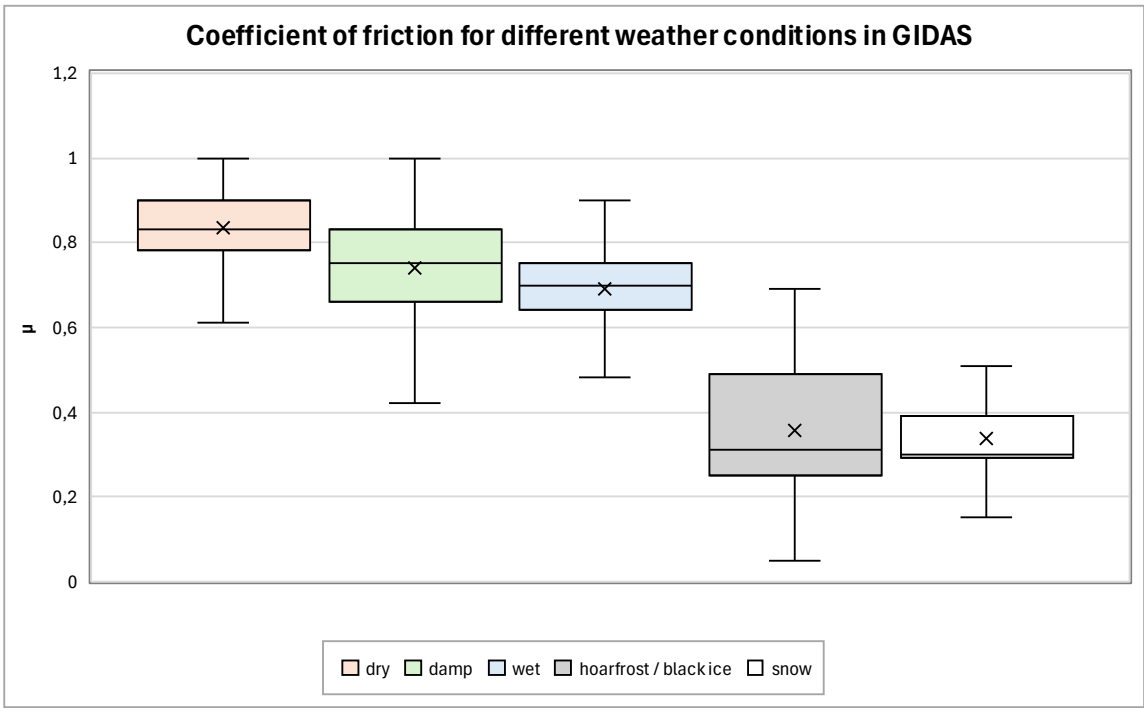

Figure 16 - Coefficient of friction for different weather conditions

The chart in Figure 16 presents a box plot analysis of the coefficient of friction (μ) under various weather conditions, based on data from GIDAS. The coefficient of friction is a crucial parameter influencing vehicle dynamics and accident outcomes, particularly under AWC.
The five categories analysed include dry, damp, wet, hoarfrost/black ice, and snow conditions. For each category, the box plot illustrates the interquartile range median, mean (marked as "×"), and range of friction coefficients observed in accident data.
Under dry conditions, the coefficient of friction is highest, with values generally ranging between approximately 0.7 and 1.0, and a mean near 0.85, reflecting optimal traction.
Damp and wet conditions show a noticeable reduction in friction, with mean values decreasing slightly from dry to damp (~0.75 to 0.8) and further under wet (~0.7). These conditions demonstrate greater variability, especially damp roads, where values can drop below 0.5.
The most significant decreases in friction are observed under hoarfrost/black ice and snow. Hoarfrost/black ice exhibits a wide range with a median around 0.3 to 0.4 and a minimum near 0.05, highlighting the extreme danger of such surfaces due to unpredictably low grip. Snow-covered roads show a similarly reduced friction profile, with median and mean values around 0.3 and reduced upper quartile limits compared to other conditions.
The clear trend observed in the chart emphasizes that as weather conditions deteriorate, the coefficient of friction declines significantly, increasing the likelihood of vehicle instability and loss of control. This highlights the importance of adaptive driving strategies and vehicle safety technologies under AWC.
To describe the selected scenarios further, the collision speeds for the scenarios were analysed. Boxplots and the distribution of them is shown in Figure 17. It shows that the Median of the collision speeds is the highest in scenario 301 with 28 km/h, while it is the lowest in scenario 302 with 14 km/h. The highest values can be found in scenario 611 with a collision speed of 106 km/h. Scenario 301 also contains a high share of accidents with higher collision speeds with 25 % of them being 44 km/h or

more. These insights are crucial for designing and evaluating ADAS and informing accident reconstruction and prevention strategies.

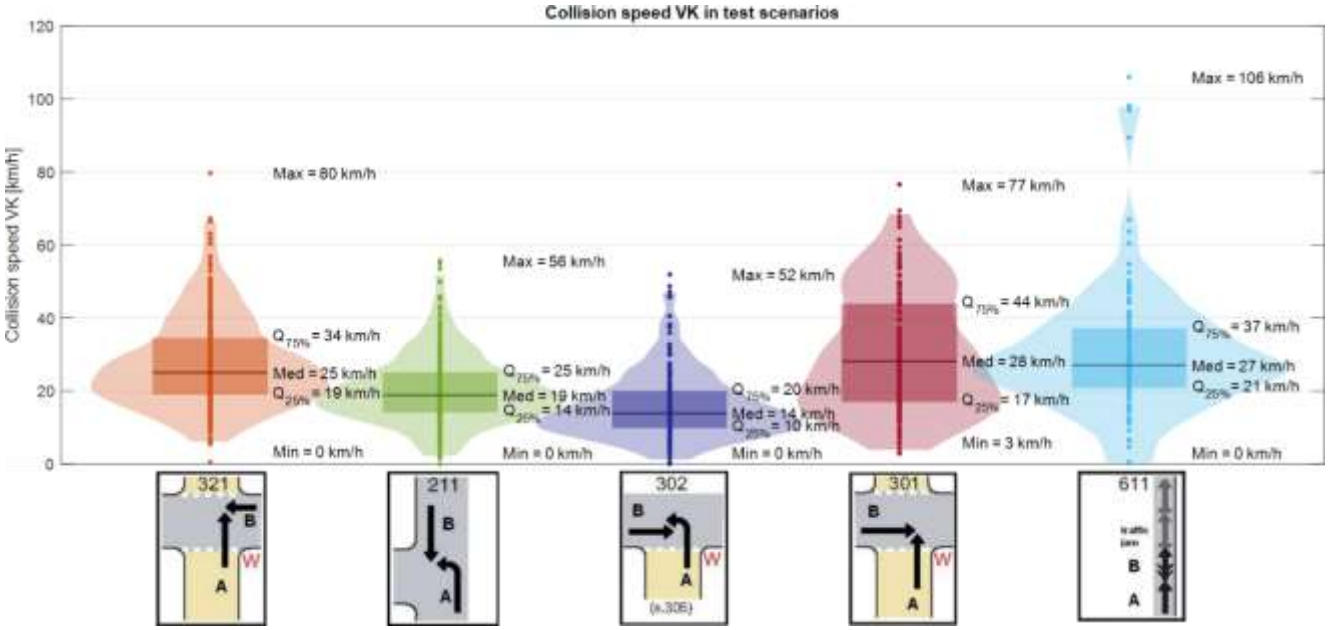

Figure 17 - Collision speeds of the vehicles that are equipped with ADAS in the different scenarios

3. Re-Simulation of selected AW scenarios

Chapter 3 describes the re-simulation of the accidents which is used to determine the effect of the AW on ADAS. It divides into two sub-chapters. The subchapter 3.1 provides an overview about the general methodology of the sensor modelling, the used influences of AW on sensors and the different ADAS configurations which are defined by the consortium. Additionally, a vehicle-to-vehicle communication (V2V) model that is used in the re-simulation is described. Subchapter 3.2 shows the results of the re-simulation. To provide a clearer understanding of the simulation and system operations, an illustrative example for a single case is presented. Furthermore, the effects of the systems are shown for each scenario.

3.1 Re-Simulation methodology

The accidents of the top 5 scenarios are re-simulated using PCM accident data as a basis. These accidents originally occurred without the influence of any ADAS. For the re-simulation, the vehicle involved in each accident is equipped with ADAS functionalities. For accidents involving two vehicles, only the vehicle identified as the cause of the accident is equipped with ADAS.

3.1.1 Modelling of Sensors

A generic, object-based sensor model is used for the sensor modelling. This is a simplification made, since sensors on the market vary significantly and there are not enough relevant parameters for a physical sensor model available. Furthermore, the existing accident data lacks environmental parameters that are necessary for a physical sensor model. The generic sensor model is described in Figure 18. It is based on the field of view of a sensor, which includes its range (r) and field of view (α). If a participant is within this field of view and is not obstructed by another object, the participant is considered as detected.

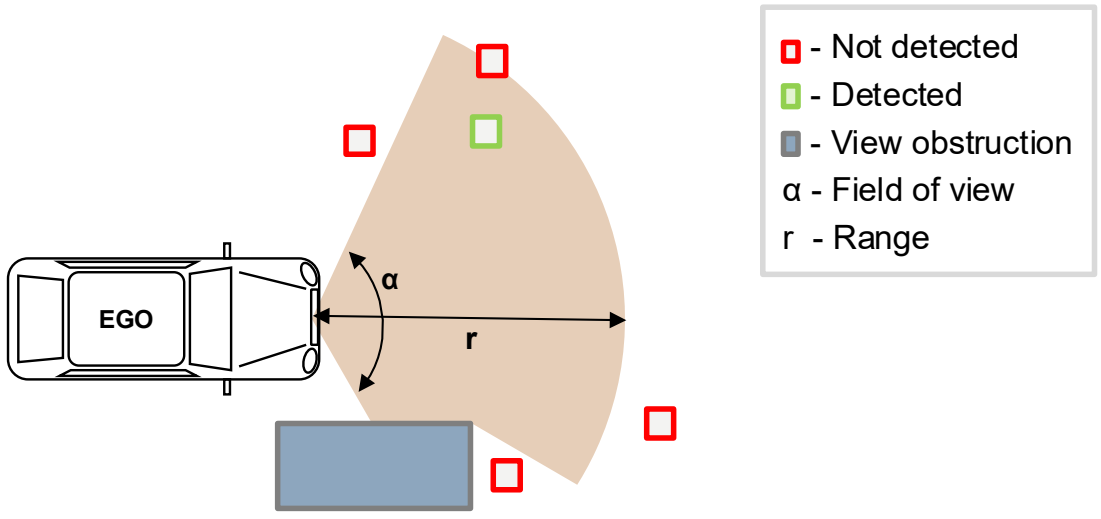

Figure 18 - Example of detection (green) for object-based sensor model

Based on the findings of Deliverable 2.2 [2] a radar and a camera are chosen as a baseline sensor configuration for the simulated vehicles. These sensors are already commonly integrated in modern vehicles. Standard ranges and field of view angles of these sensors are shown in Table 3.

Table 3 - Baseline range and field of view angle values for camera and radar under good weather conditions

	Range	Field of view angle
Camera	150 m	120°
Radar	300 m	120°

The standard ranges describe the ranges of the sensors for cars and trucks. For other types of road users these values are reduced based on the available technical data of the radar "Continental ARS 404" [3]. The data suggests a reduction of the sensor range to 80 % of the maximum range for motorcycles; 60 % for bicycles/mopeds and 40 % for pedestrians. These values are applied to both sensors.

3.1.2 Influence of AWC on Sensors

The influence of AWC on sensor ranges is derived from the sensor impact analysis detailed inDeliverable 2.2. [2] These influences are shown in Table 4. A scale from "1" to "3" is used, where "1" indicates a severe impact and "3" represents a negligible impact.

Table 4 - Impact of weather on sensors. (1 severe impact, 2 moderate impact, 3 negligible impact)

Condition	Radar	Camera
Fog	3	1
Rain - Light and moderate	3	2
Rain - Heavy	2	1
Snow	3	1
Spray/Splash effect	3	1
Lighting effects	3	1
Temperature	3	3
Object surface state	3	2
Sensor surface state	2	1
Sensor weather capacity	**3**	**1**

Based on these values and the combined experience of the AWC consortium members, the resulting reductions of ranges in AWC are determined. These reductions combined with additional sensor range reductions that depend on the type of the opposing road user in the accident.

Table 5 - Influence of AWC on the camera range

Condition	Condition detailed	Camera range
Normal	-	100 %
Fog	No visibility information	60 %
Fog	Visibility 100 m	35 %
Fog	Visibility 200 m	70 %
Fog	Visibility 300 m	95 %
Rain	Light and moderate [30 mm/h]	75 %
Rain	Heavy [80 mm/h]	45 %
Snow	-	30 %
Lighting effects	-	30 %

Table 5 shows the impact of AWC on the camera range used in the simulations. For normal fog conditions with no further specifications the camera range is set to 60 %. If the visibility is known, the range is reduced to 35 % of the visibility value. In rainy conditions, the camera range is reduced to 75 % for light and moderate rain, and to 45 % for heavy rain. During snow and in the presence of glare or lightning effects, the camera range is reduced to 30 %.

Table 6 Influence of AWC on the radar range

Condition	Condition detailed	Radar range
Normal	-	100 %
Fog	No visibility information	100 %
Fog	Visibility 100 m	100 %
Fog	Visibility 200 m	100 %
Fog	Visibility 300 m	100 %
Rain	Light and moderate [30 mm/h]	100 %
Rain	Heavy [80 mm/h]	75 %
Snow	-	100 %
Lighting effects	-	100 %

presents the influences of AWC on the radar sensor range used in the simulations. Since radar is less affected by AWC than the camera, there is only a reduction to 75 % for heavy rain.

3.1.3 CONFIGURATIONS OF ADAS

In order to assess the safety benefits of ADAS, three different system configurations are modelled in the simulation. The first configuration, called “standard ADAS”, simulates an active emergency braking system that applies braking input to the vehicle to avoid a collision. The sensors of the standard ADAS are affected by the AWC as described in sub-chapter 3.1.2. Additionally, the ADAS assumes a possible deceleration of 8.5 m/s^2 and times its intervention accordingly. However, the system is not aware of the current coefficient of friction available at that time. After a buildup time of 0.15 s (Figure 19), braking is conducted with the maximum deceleration, that is possible with the available coefficient of friction. This can be lower than the anticipated 8.5 m/s^2, which can compromise the system.

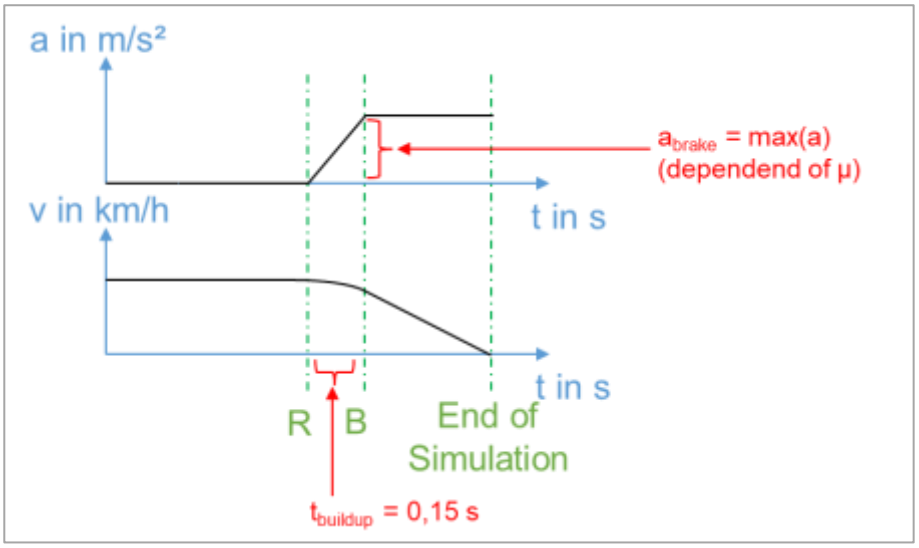

Figure 19 - Modelling of ADAS intervention with the reaction of the system “R” and the start of the full braking “B”

The second ADAS version is called “robust ADAS”. Unlike the standard ADAS, the robust ADAS is able to estimate the current available coefficient of friction and adjust the timing of its braking input accordingly. Nevertheless, its sensors remain affected by the weather conditions. The results of this ADAS version compared to the standard ADAS represent the influence of friction in AWC.
A third configuration, called the “optimal ADAS”, is modelled to demonstrate the maximum potential of ADAS under AWC. Similarly to the robust ADAS, the optimal ADAS can estimate the coefficient of friction and adapt the braking input. Additionally, the sensors are not affected by the AWC. The results of this ADAS version compared to the robust ADAS represent the influence of the perception in AWC in combination with the friction detection.

Additionally, to the three ADAS configurations described above, a set of simulations is conducted to determine the influence of sensor perception alone – without friction estimation.

3.1.4 V2V MODELLING

In addition to the different ADAS configurations, a V2V is modelled. For this purpose, the “Free-Space-Pathloss-Model” - an empirical approach to calculate the Received Signal Strength Indicator (RSSI) - is used. This model is influenced by the line of sight between vehicles but has no direct consideration of physical damping or reflection effects. The calculation of the RSSI is shown in Figure 20.

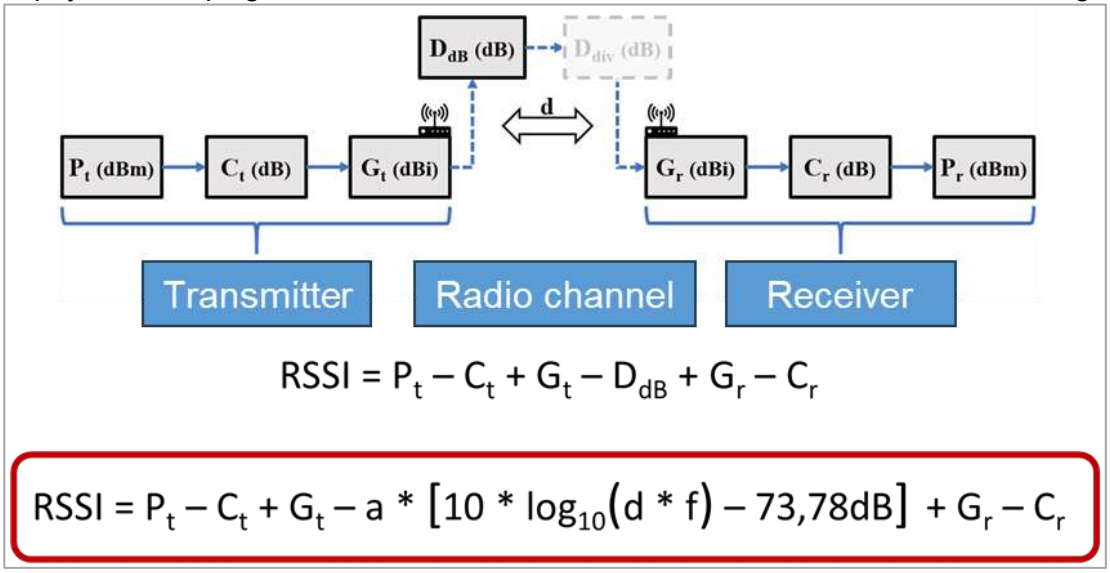

Figure 20 - Free-Space-Pathloss-Model of the RSSI calculation for the V2V communication

The parameters used for the calculation are described in Table 7. The line losses of the transmitter and receiver are 3.0 dB. The antenna gains for both are assumed to be 8.0 dBi. A transmit power of 23 dBm is used as well as a radio frequency of 5.875 GHz. During line-of-sight conditions of the two vehicles, a path loss factor of 2.7 is used, while 2.0 is used during conditions without line of sight. The distance between the vehicles at each timestep in the PCM is measured using the distance between their centres of gravity.

Table 7 - Used parameters for Free-Space-Pathloss-Model

Parameter	Description	Used values
C_t	Line losses (transmitter)	3.0 dB
C_r	Line losses (receiver)	3.0 dB
G_t	Antenna gains (transmitter)	8.0 dBi
G_r	Antenna gains (receiver)	8.0 dBi
P_t	Transmit power	23 dBm
f	Radio frequency	5.875 GHz
a	Path loss factor	2.7 (line of sight) / 3.0 (no line of sight)
d	Distance	*From PCM data in each timestep*

The results of the RSSI calculations are displayed in Figure 21 for line-of-sight and non-line-of-sight conditions. A threshold of -90 dB is used, up to which a communication between the two vehicles is

possible. Therefore, it is assumed that for line-of-sight conditions a communication up to 145 m and for obstructed non-line-of-sight conditions a communication up to 51 m is possible.

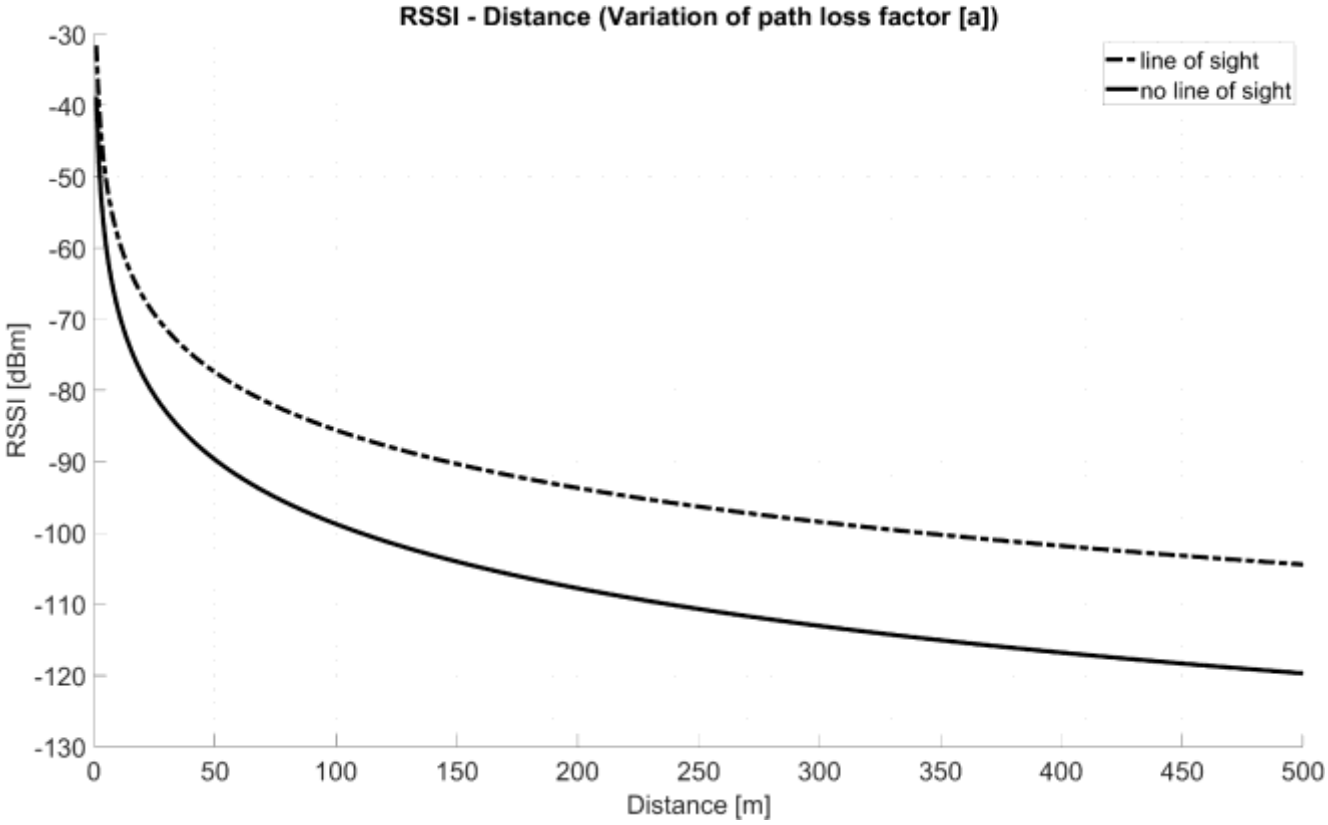

Figure 21 - RSSI dependent on the distance of the vehicles

If communication is possible, the V2V-model calculates the time to collision (TTC) for each timestep. The system warns the driver at the last timestep when the TTC exceeds 1.7 s. In response, the driver's reaction is modelled as a braking input after a reaction time of 1.1 s. Following this, a buildup time of 0.15 s is applied, after which the driver brakes with the maximum possible deceleration, as illustrated in Figure 22. [4]

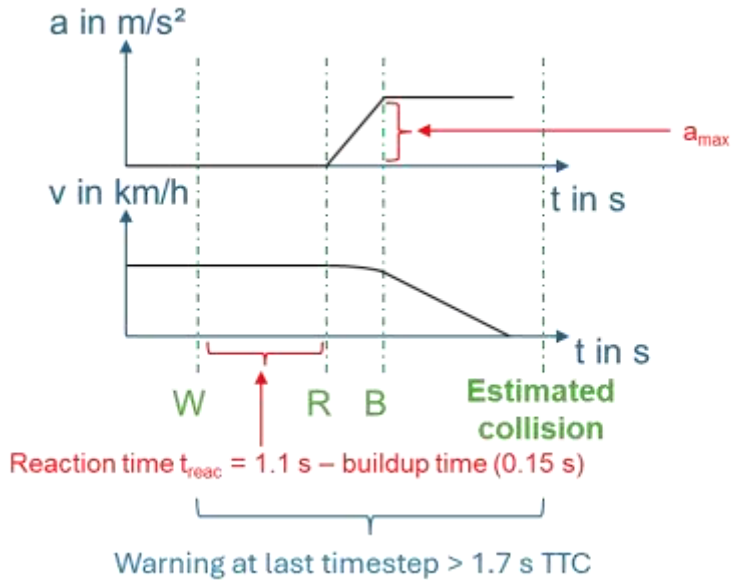

Figure 22 - Schema of modelled ADAS braking interaction with the warning timestep "W" the reaction of the driver "R" and the start of full braking "B"

3.2 RESULTS OF RE-SIMULATION

The results of the re-simulation are presented in the following chapter, along with an analysis of the avoided accidents for the different ADAS configurations.

3.2.1 EXEMPLARY SINGLE CASE RESULTS

The outcome of the simulation differs depending on the vehicle constellation in the simulated cases. Even a perfectly working ADAS cannot prevent all collisions, as sensor limitations – such as incomplete environmental coverage or obstructions – can impair detection. This is particularly evident in scenarios 321, 302 and 301, where the other vehicle is coming from the side.

An example of a collision in scenario 211 is illustrated in Figure 23. In this particular case the passenger vehicle(red) is coming from the right side and is turning to the left. A bicycle is coming from straight ahead and they collide. Although there is no precipitation during the accident, the road is wet, resulting in a coefficient of friction of 0.61 for the vehicle.

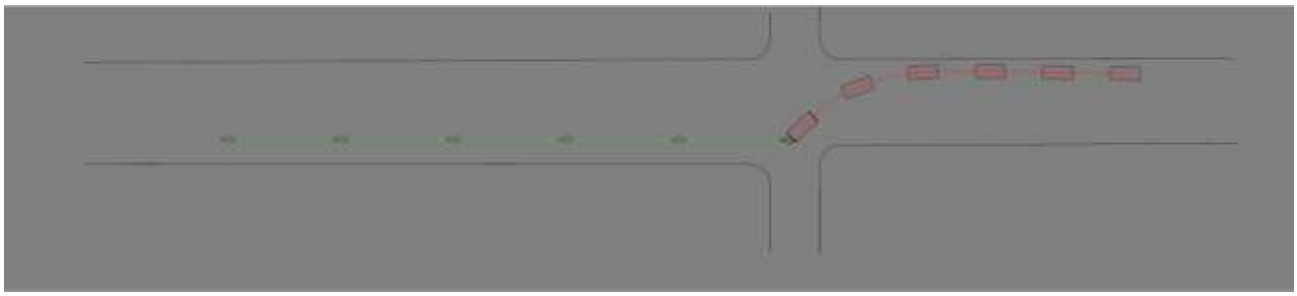

Figure 23 - Example accident case of scenario 211 (participants are shown every 1 second ant in the collision position)

A re-simulation of the accident with the standard ADAS is shown in Figure 24. The cameras detection range for bicycles, which is 90 m, is indicated in red. The bicycle is detected at the beginning of the simulation. The vehicle starts to brake at 4.2 s. Due to the low coefficient of friction, the vehicle is unable to achieve the needed deceleration of 8.5 m/s², and the collision cannot be avoided.

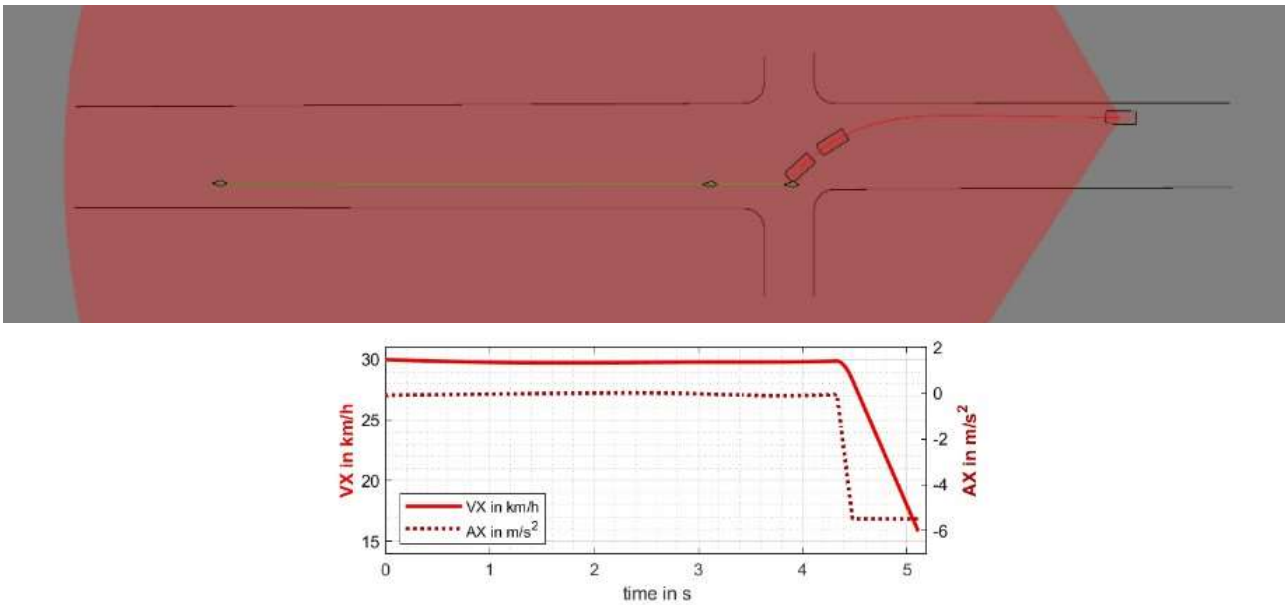

Figure 24 – Re-simulation of example accident case with standard ADAS (participant are shown at the beginning, at the timestep where the ADAS starts to break and in the collision position)

Figure 25 shows the re-simulated accident with the robust ADAS. Unlike the standard ADAS, the robust ADAS estimates the available coefficient of friction and initiates braking earlier, at approximately 4.1 s. Although the deceleration rate is the same as with the standard ADAS, the earlier braking allows the vehicle to avoid the collision with the bicycle.

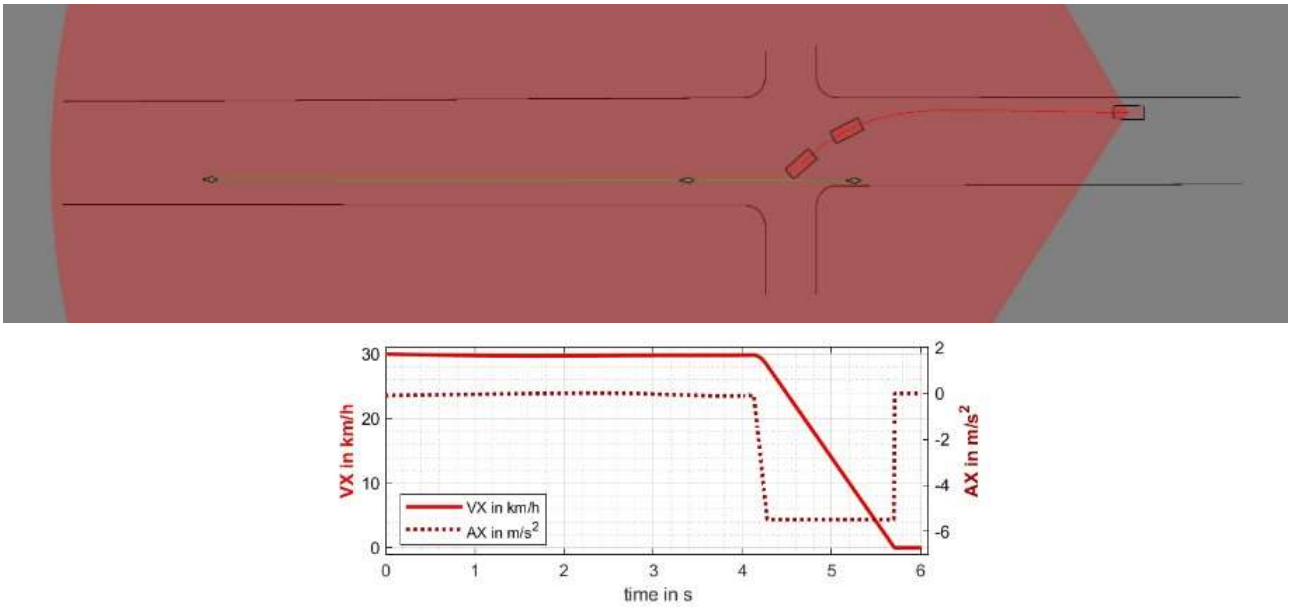

Figure 25 – Re-simulation of example accident case with robust ADAS (participant are shown at the beginning, at the timestep where the ADAS starts to break and in the end position)

There is no difference between the optimal ADAS and the standard ADAS due to the fact that the bicycle is detected by the sensor all the time, so a bigger range doesn't have an influence.

3.2.2 Overall result of ADAS configurations

All accidents of the top five scenarios are simulated with the three different ADAS configurations. The results are summarized in Figure 26. With the standard ADAS, 24.8 % of the accidents with AWC could be avoided in scenario 302, which is the lowest among all scenarios. It is followed by scenario 611 with 27.8 % avoided accidents, scenario 301 with 30.2 % avoided accidents and scenario 321 with 31.9 % avoided accidents. With the standard ADAS, the highest number of accidents are avoided in scenario 211, with 38.8 %.
With the robust ADAS, an additional 13.1 % (scenario 302) to 69.0 % (scenario 611) of accidents could be avoided. The robust ADAS roughly doubles the avoidance rate of the system.
The optimal ADAS does not avoid additional accidents in the scenarios 302 and 301. In the remaining scenarios, it can prevent between 0.5 % (scenario 321) and 1.6 % (scenario 611) accidents. Compared to the robust ADAS, the additional effect of the optimal ADAS is relatively small.

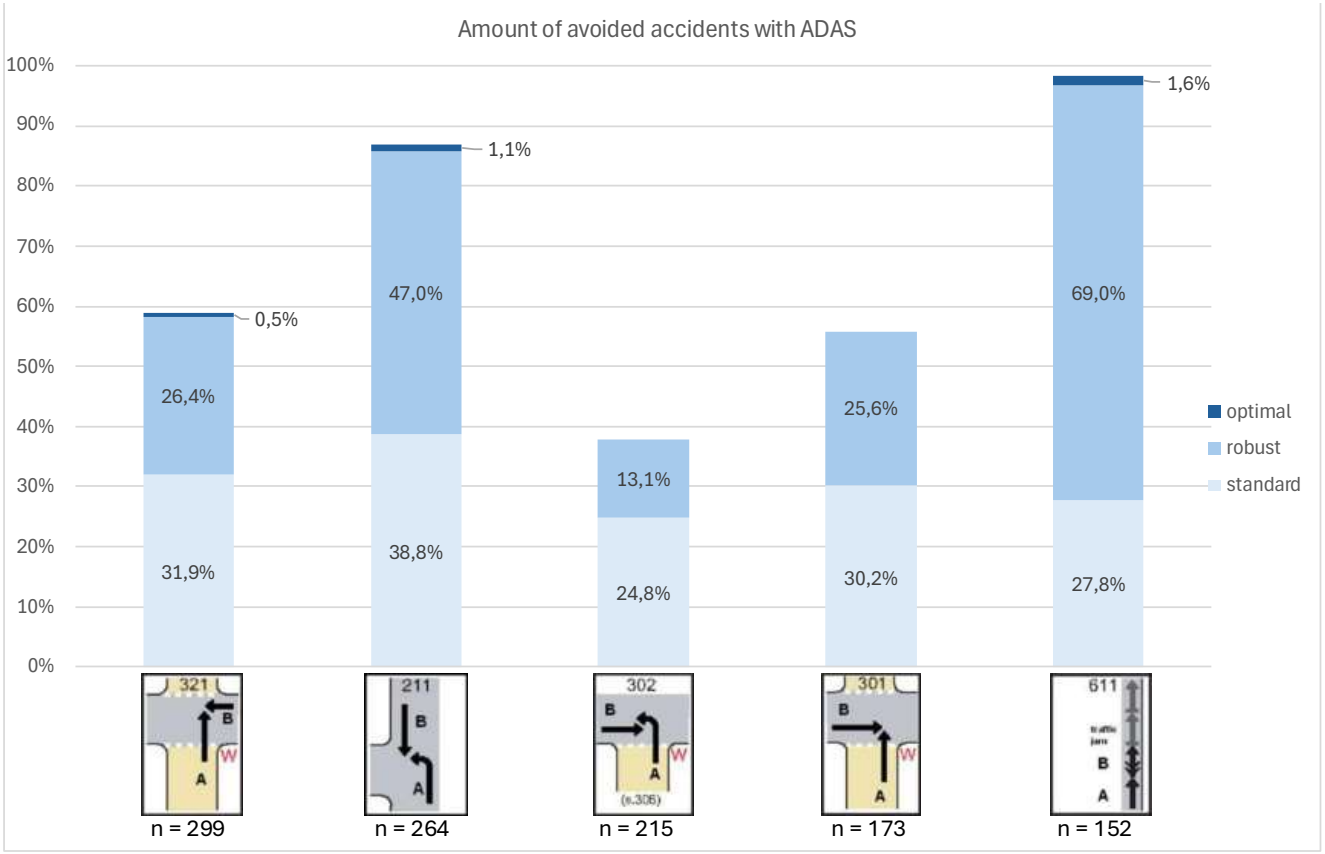

Figure 26 - Number of avoided accidents for each scenario and ADAS configuration

To better understand the systems, the distances of both participants at the moment the ADAS starts braking are shown in Figure 27. This figure shows boxplots with the 25th percentile, Median and 75th percentile as well as the minimum and maximum values of these distances. Behind the boxplots the distribution of the distances is visualized. The median of the robust ADAS is 0.8 m greater than the median of the standard ADAS, indicating that the system brakes earlier due to its awareness of the available friction. The boxplot of the optimal ADAS appears similar to the robust ADAS, which explains their comparable performance. A key difference is visible in the maximum values, which are higher due to the extended sensor range.

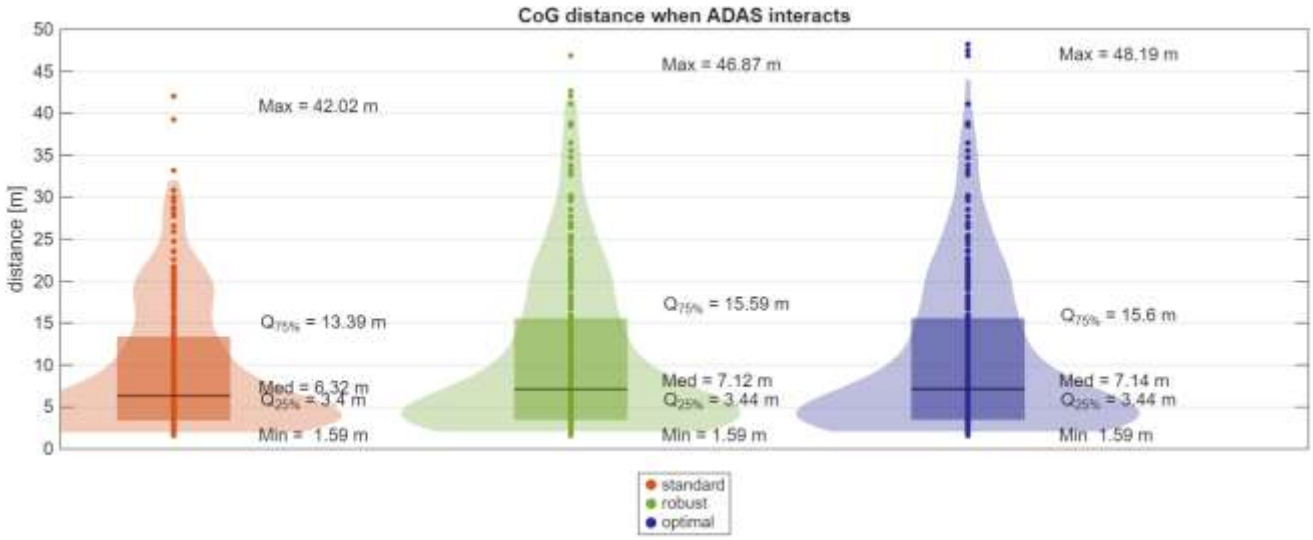

Figure 27 – CoG distance of the participants in the accident when the ADAS starts to interact for each ADAS configuration for scenario 321

The distribution of the TTC values of the moment when the ADAS starts braking is pictured in Figure 28 and shows similar tendencies. While comparing the robust ADAS to the optimal ADAS, only minor differences can be observed in the maximum values. The TTC median shows an increase of nearly 0.1 s from the standard ADAS to the robust and optimal ADAS. The maximum TTC increases by 0.77 s for the robust and optimal ADAS. This indicates a very early braking input, which is possible in the simulation of the systems. Since the braking input is applied very early, it cannot be guaranteed that such behaviour would occur in a real-world application, as this could lead to a high amount of false positives in the system.

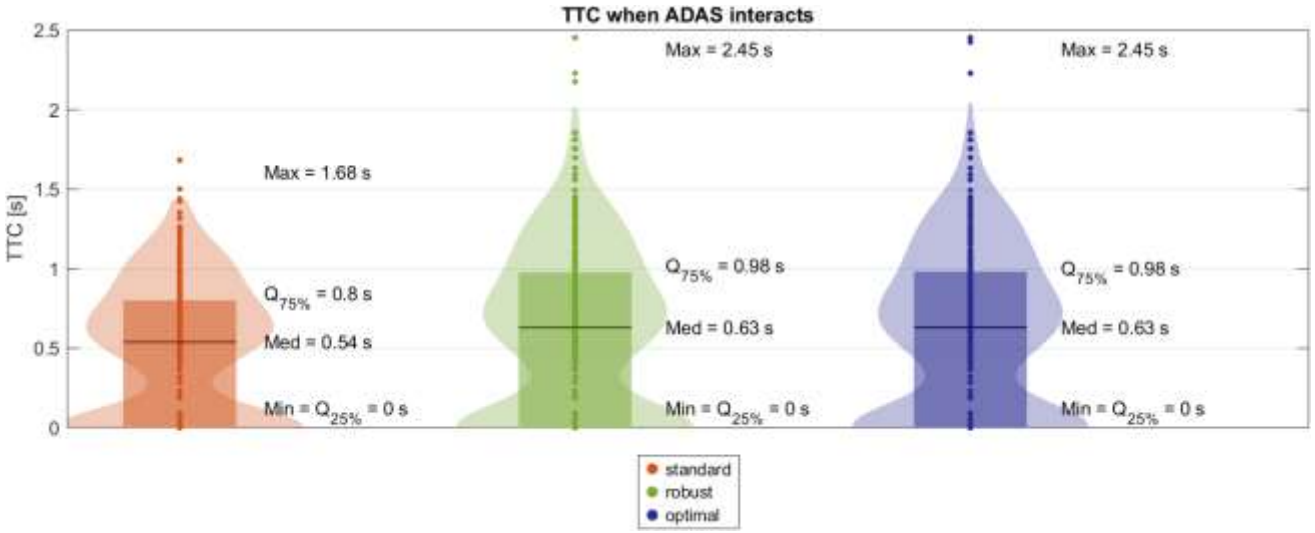

Figure 28 - TTC when the ADAS starts to interact for each ADAS configuration for scenario 321

The TTC values grouped by collision occurrence are visualized in Figure 29. The values for the standard ADAS configuration in scenario 321 are shown. For the accidents where the collision could not be avoided the TTC values are much lower than in the accidents where the collision could be avoided. A high amount of accidents have a TTC value of 0 s, which means that the ADAS did not intervene, because the sensors did not detect the opponent.

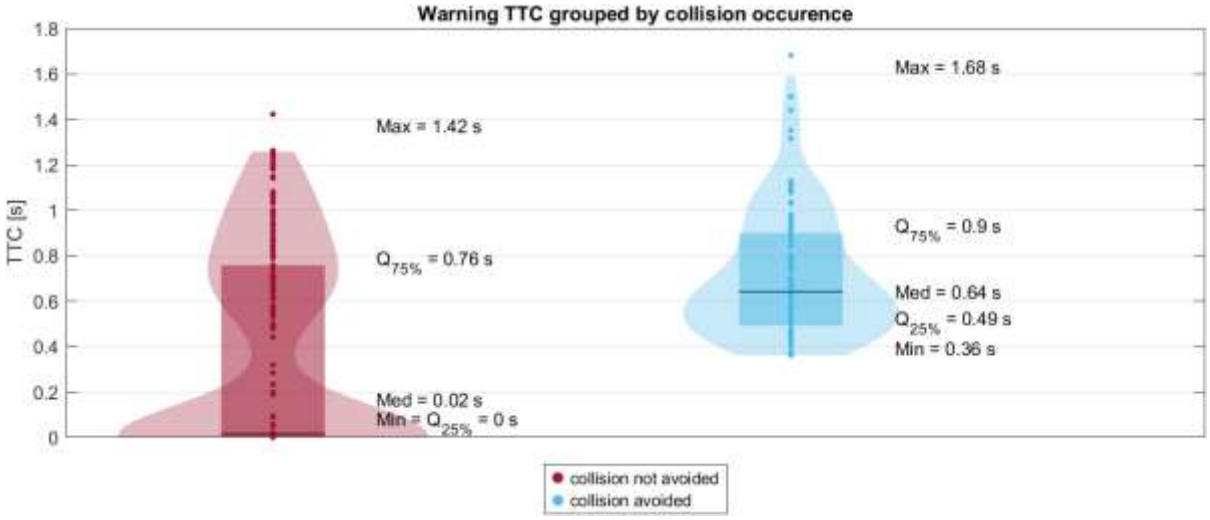

Figure 29 - TTC when the ADAS starts to interact grouped by collision occurrence for scenario 321 and with the standard ADAS configuration

While this study is focussing on the number of avoided accidents, there is also a mitigation effect in accidents that cannot be prevented. This is displayed in Figure 30, which shows the distribution of the collision speeds. The median of the collision speeds is lowered by 6.3 kph, and the maximum could even be reduced by 15.2 kph. This reduction could significantly decrease the risk of injuries for the individuals involved in the accident.

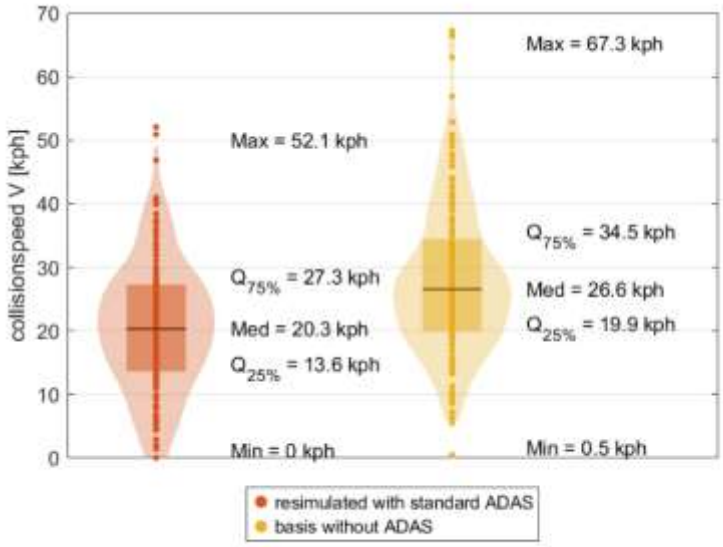

Figure 30 Collision speeds in accidents, where the accident can't be avoided (68,9 %) in scenario 321 with standard ADAS

3.2.3 ISOLATED EFFECT OF FRICTION DETECTION

The isolated effect of friction detection in the ADAS can be seen in Figure 31. The effect of the friction detection compared to the standard ADAS is the same as the robust ADAS since it is the only difference to the standard ADAS. On average, 36.2 % of additional accidents could be avoided with the friction detection. The significant effect can be attributed to the high proportion of cases – over 80 % in most scenarios - with a wet, damp or icy road condition, as shown in Figure 15.

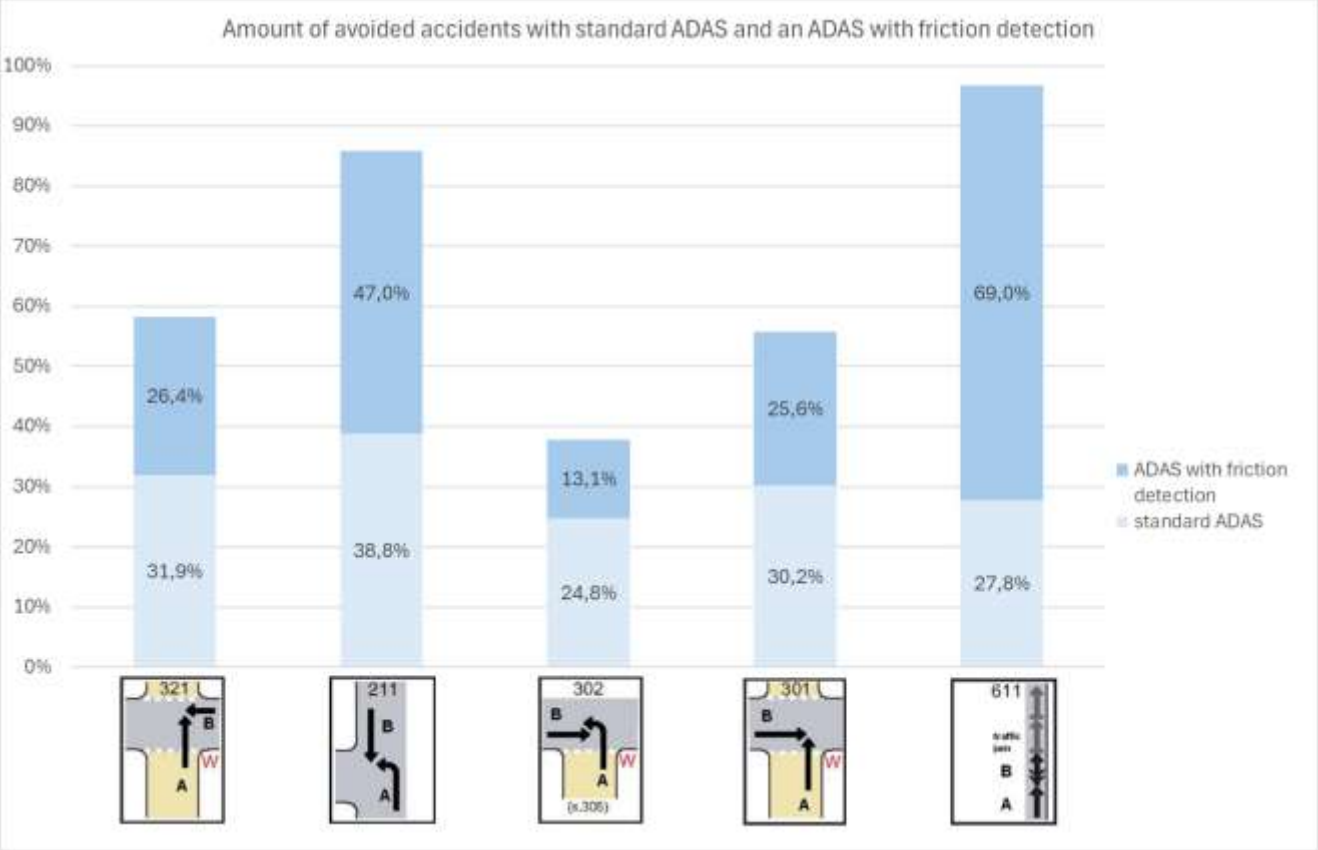

Figure 31 – Isolated effect of friction detection

3.2.4 ISOLATED EFFECT OF PERCEPTION

The isolated effect of optimal perception in the ADAS can be seen in Figure 32. This effect differs compared to the optimal ADAS, since it shows the isolated effect, while the optimal ADAS combines both optimal perception and friction detection. The optimal perception has an added effect only in scenario321 (0.3 %) and scenario 211 (0.8 %). In the other three scenarios, there is no additional effect. The relatively low impact can be explained by the small number of accidents involving precipitation (Figure 13) and sun glare (Figure 14), which affects sensor precipitation. Additionally, the influence of weather conditions on the sensors used in the simulation is not strong enough to have a valuable impact on the perception. In all of the accidents, the impact on the camera is greater than on the radar. Even under the most severe perception limitations - such as snow or lighting effects - the camera's detection range for passenger vehicles is reduced to 45 m, compared to the baseline of 150 m. In the most re-simulations, this reduced range is still sufficient to detect the opponent in time and avoid a collision.

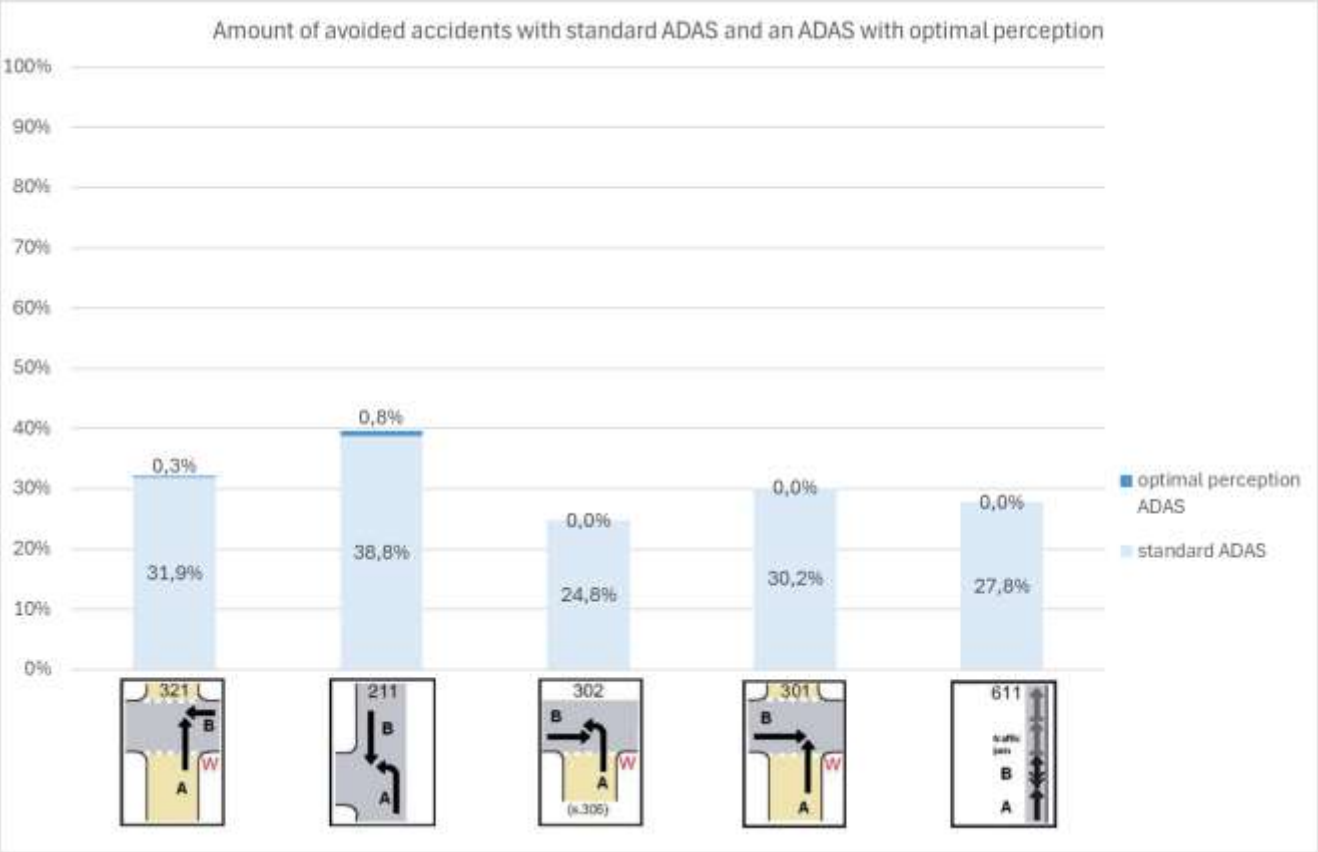

Figure 32– Isolated effect of optimal perception

3.2.5 EFFECT OF V2V

In addition to the three different ADAS configurations, a V2V-system is modelled and combined with the standard ADAS. The simulations were conducted for the scenario 321, as it is the most frequent accident scenario, and scenario 611, since there is a relatively simple implementation possible. Nevertheless, the results provide an indication of the potential of connected systems compared to sensor-based ADAS.

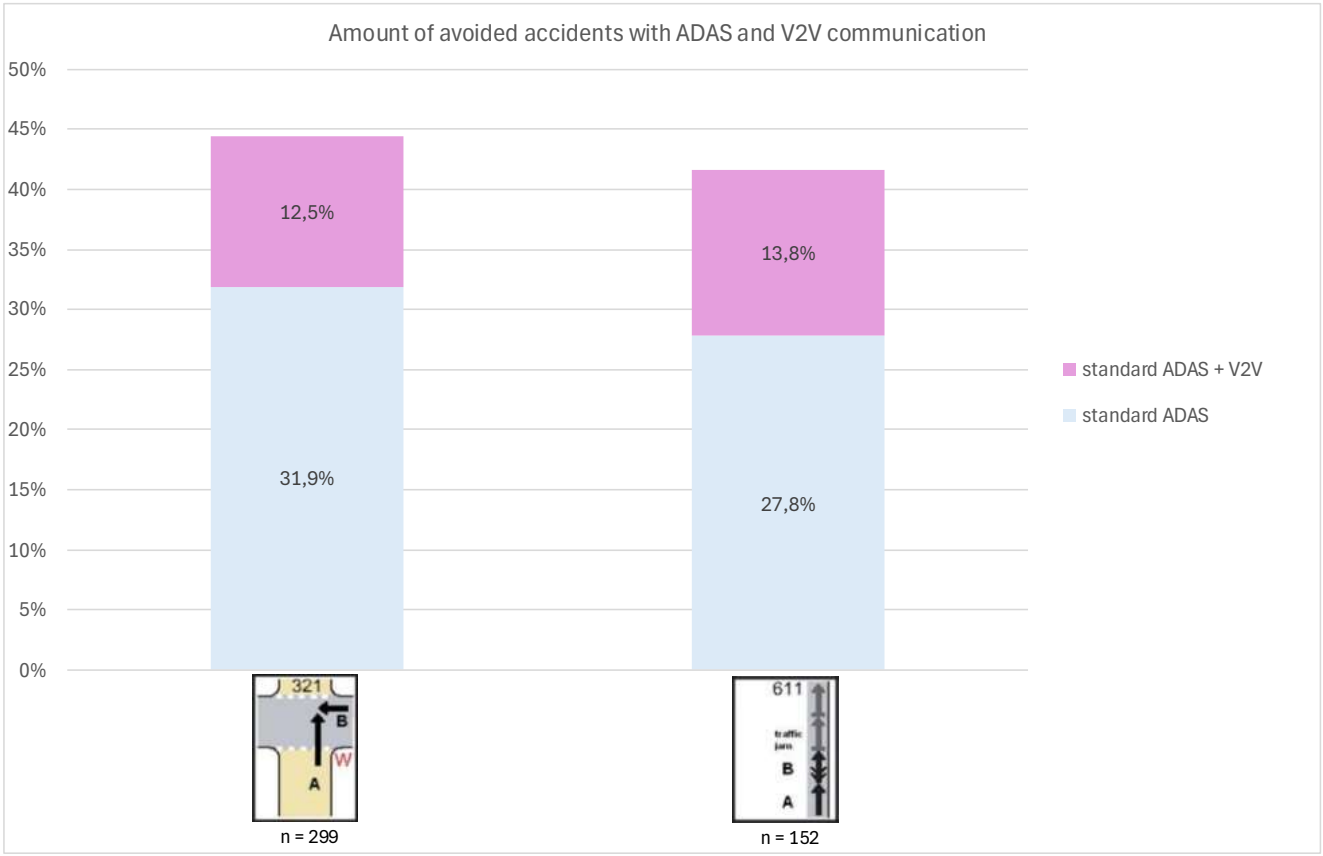

Figure 33 - The added effect of V2V communication to ADAS

The effect of added V2V-communication is shown in Figure 33. In scenario 321, 12.5 % more accidents could be avoided compared to the standard ADAS. In scenario 611, V2V communication led to an addition of 13.8% of avoided accidents compared to the standard ADAS. These results suggest that incorporating V2V-communication could be beneficial in AWC scenarios.

4. Summary and outlook

The main objective of the study is to assess the safety potential of improving ADAS/AD functionality in AWC. The relation to other work packages is outlined with the key inputs for specific accident scenarios from WP1 and with the influence of AW on sensors from WP2. The impact of AW on accidents is described, and the GIDAS scenarios that occurred most frequently under AWC were selected. LOC-accidents were excluded from this selection due to their decreasing relevancy. The GIDAS PCM cases from the top 5 scenarios are chosen for re-simulation, and the distribution of weather conditions for these cases is presented.
Following that the re-simulation process is described. An object-based sensor model camera and radar is developed, incorporating limitations on perception ranges for various weather conditions. The ADAS model and its functionality is described, along with different configurations used in the simulation. Additionally, the V2V-model applied in some simulations is characterized. In the end, the results of the different ADAS configurations across the top 5 scenarios are presented, as well as key parameters, which describe system behaviour.
The results show that the standard ADAS can avoid between 24.8 % and 38.8 % of the accidents with AW, depending on the scenario. A robust ADAS capable of detecting the current coefficient of friction can prevent an additional 13.1 % to 69.0 %, more than doubling the number of avoided accidents. This improvement is achieved through earlier braking at a higher TTC. Friction detection is of particular relevance because most of the accidents with AWC include affected road conditions.
An optimal ADAS, which combines the detection of friction with weather-resilient sensors, has only a minor effect between zero and up to 1.6 % of additional avoided accidents. This is due to the relatively low number of accidents involving precipitation and the limited impact of AW on sensor performance in the simulation. The isolated effect of optimal perception without the friction detection is even lower, ranging from zero to 0.8 % of additional avoided accidents. V2V-communication also shows potential in AWC-related accidents, enabling approximately 13 % more avoided accidents compared to the standard ADAS. This benefit is achieved due to the earlier braking by the warned driver.

Overall, the simulation results highlight the strong influence of the coefficient of friction and its detection on the ADAS performance. This indicates that accurate detection and implementation of the coefficient of friction can double the amount of avoided accidents under AWC. Perception plays only a minor role in ADAS performance in accidents. However, in autonomous driving, perception has a critical impact on system effectiveness and safety during AWC. These findings need to be validated on the test track with real systems to prove that the assumptions and parameters which are used in the simulation reflect real-world conditions.

5. Acknowledgements

The WeatherSafe consortium would like to acknowledge for their support and work all the Partners and Third Parties involved:



6. List of illustrations

Figure 1 - Analysis of weather parameters and results of WP1 [1] 8
Figure 2 - LOC accidents and their presence of skidding 9
Figure 3 - Distribution of road surface conditions and precipitation in LOC accidents 10
Figure 4 - Number of LOC accidents under AWC over the past years 11
Figure 5 - Collision speed of participants of loss of control accidents 12
Figure 6 - Collision speed of participants of intersection accidents 12
Figure 7 - Distribution of accidents which are caused by the participant exceeding the speed limit 12
Figure 8 - Top five accident scenarios for re-simulation 14
Figure 9 - Top five AW KSI accident scenarios 16
Figure 10 - Traffic accident scenario as first sketch 18
Figure 11 - Simulated accident scenario as trajectory in the PCM 18
Figure 12 - Top five AWC scenarios and their number of cases in the GIDAS-PCM 19
Figure 13 - Distribution of precipitation in the top five PCM scenarios 19
Figure 14 - Distribution of sun glare in the top five PCM scenarios 19
Figure 15 - Distribution of road surface conditions in the top five PCM scenarios 19
Figure 16 - Coefficient of friction for different weather conditions 20
Figure 17 - Collision speeds of the vehicles that are equipped with ADAS in the different scenarios 21
Figure 18 - Example of detection (green) for object-based sensor model 22
Figure 19 - Modelling of ADAS intervention with the reaction of the system “R” and the start of the full braking “B” 25
Figure 20 - Free-Space-Pathloss-Model of the RSSI calculation for the V2V communication 26
Figure 21 - RSSI dependent on the distance of the vehicles 27
Figure 22 - Schema of modelled ADAS braking interaction with the warning timestep “W” the reaction of the driver “R” and the start of full braking “B” 28
Figure 23 - Example accident case of scenario 211 (participants are shown every 1 second ant in the collision position) 29
Figure 24 – Re-simulation of example accident case with standard ADAS (participant are shown at the beginning, at the timestep where the ADAS starts to break and in the collision position) 29
Figure 25 – Re-simulation of example accident case with robust ADAS (participant are shown at the beginning, at the timestep where the ADAS starts to break and in the end position) 30
Figure 26 - Number of avoided accidents for each scenario and ADAS configuration 31
Figure 27 – CoG distance of the participants in the accident when the ADAS starts to interact for each ADAS configuration for scenario 321 32
Figure 28 - TTC when the ADAS starts to interact for each ADAS configuration for scenario 321 33
Figure 29 - TTC when the ADAS starts to interact grouped by collision occurrence for scenario 321 and with the standard ADAS configuration 33
Figure 30 Collision speeds in accidents, where the accident can’t be avoided (68,9 %) in scenario 321 with standard ADAS 34
Figure 31 – Isolated effect of friction detection 35
Figure 32– Isolated effect of optimal perception 36
Figure 33 - The added effect of V2V communication to ADAS 37

7. List of tables

Table 1 - Detailed weather conditions during the top five AWC scenarios without LOC 15
Table 2 - Detailed weather conditions during the top five KSI scenarios without LOC 16
Table 3 - Baseline range and field of view angle values for camera and radar under good weather conditions 23
Table 4 - Impact of weather on sensors. (1 severe impact, 2 moderate impact, 3 negligible impact) . 23
Table 5 - Influence of AWC on the camera range 23
Table 6 Influence of AWC on the radar range 24
Table 7 - Used parameters for Free-Space-Pathloss-Model 26

8. References

[1] T. Weber (VUFO), „[D1.1/1.2] - Assessment of ADAS/AD Peformances under adverse weather conditions,“ Dresden, 2024.

[2] Michael Graf (CARISSMA), „[D2.2] - Assessment of ADAS/AD Peformances under adverse weather conditions,“ 2024.

[3] R. Liebske, *Short Description ARS 404-21 (Entry) + ARS 408-21 (Premium) Long Range Radar Sensor 77 GHz - Technical Data,* Version 1.01 en Hrsg., Continental, Hrsg., 2016.

[4] K. R. Marcus Petzold, *Potentialbewertung zukünftiger V2X-Lösungen in PKW-Fahrrad-Unfällen,* 2024.